Quantification of the Gas and Liquids in Place and Flow Characteristics of Shale and other Fine-Grained Facies in Western Canada

results of research

final report to Geoscience BC, April 2019

Geoscience BC Report: 2019-06

R. Marc Bustin

A. A. M. Bustin, S. Hazel, A. Hosseinian, M. LeMessiuer, E.A. Letham,

M. Longobardi, E. Munson, J. Owen, T. Wilson, P. L. Silva

The University of British Columbia

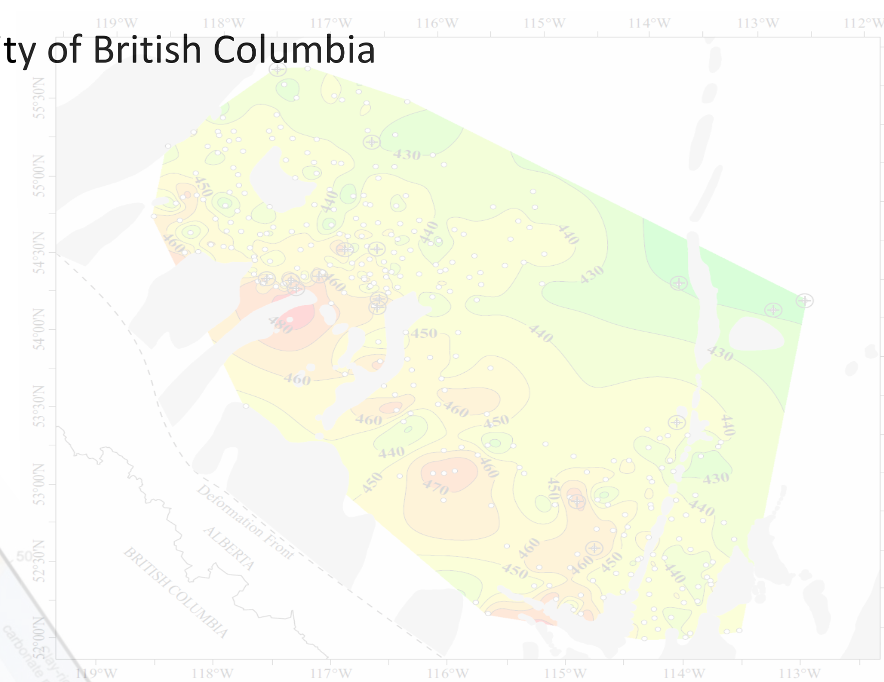

Contents

Executive Summary ... 3

Acknowledgments ... 6

Introduction and Background ... 7

Results ... 8

a) Quantifying gas and liquid hydrocarbons in place and flow characteristics of shale gas and oil reservoirs ... 8

i. Insights into pore structure characterization and permeability measurement of fine-grained sedimentary reservoir rocks in the laboratory at reservoir stress states ... 8

ii Importance of tortuosity and asperities on fracture permeability in shales. ... 11

iii. Measuring liquid permeability, multiphase flow, and relative permeability in ultra tight rocks ... 12

iv Controls and variability of the flowback water inorganic chemistry and rheology of the Montney Formation ... 13

v. Retained liquids in place in shale and other fine-grained facies- impact of imbibition of oil based mud on core based oil saturations ... 19

b) Gas in place and flow characteristics of fine-grained facies in Western Canada. ... 22

i. Regional Variation in Organic Maturation and Gas Composition ... 22

ii Petroleum system analyses of Upper Devonian organic rich shales of the Horn River and Liard Basins, Cordova Embayment, and adjacent parts of the Western Canadian Sedimentary Basin ... 30

iii Reservoir Characterisation of the Duvernay Formation, a pore to basin scale study ... 37

iv Petroleum System Analyses of the Doig Formation, Northeastern British Columbia ... 52

References ... 59

Executive Summary

Rapid growth of the unconventional shale gas and shale oil industry has outpaced our understanding of the processes that determine gas and liquids in place as well as our methods for quantifying flow characteristics of the rocks, particularly when multiple phases are present. A three year research program was undertaken at The University of British Columbia with the overall goal of better understanding the occurrence of liquid hydrocarbons in shales and the factors that contribute to their producibility.

The project had two interrelated objectives: a) quantifying gas and liquid hydrocarbons in place and flow characteristics of shale gas and oil reservoirs; and b) quantifying gas in place and flow characteristics of fine-grained facies in Western Canada. In this report the salient results, conclusions, and interpretations are provided. References are provided to the fully detailed reports, graduate student theses, and papers.

Shales, in comparison to conventional petroleum reservoirs, are unique in their fine-grained nature and resulting nano- to micrometre scale pore systems. Characterising pore systems is important as they are the location of both storage and transport of hydrocarbons. The geometry of the pore systems and composition of the pore walls influence hydrocarbon production through capillarity and permeability, and by factors recently recognized including pore size-dependent phase envelopes in nanometer scale pore and capillary condensation. The methodologies currently used to characterize the pore systems, hydrocarbon storage capacity, and flow characteristics of the shale matrix are mainly a hybrid mixture of specialised methods used for coals and conventional reservoir rocks and have been applied to shales with limited consideration of their unique and varied properties or the physics of extremely small places. In our study, we developed new methods and refined existing methods to better characterise the pore structure, permeability, and mineralogy of find grained reservoirs. Our research shows that Klinkenberg slip extends to much high pressures than previously considered and we show how slippage measurements can be used to characterise the pore structure. We have developed a method of measuring effective permeability of fine-grained reservoir rocks at different fluid saturations using ethane gas at a range of pore pressures up to the saturated vapour pressure. An instrument and algorithms were developed to measure liquid permeability by pulse decay with determination of the relative permeability for ultra-low permeability rocks. The study of sample preparation for mineralogy by X-ray diffraction has resulted in the development of a protocol that greatly reduces the time required in sample preparation without compromising accuracy of the results. Similarly, we have refined methods of characterising capillary pressures with mercury intrusion porosimetry data through developing better algorithms for correcting for sample conformance and compressibility.

To understand the change in fracture permeability with production, we investigated fracture closure with declining pore pressure. The importance of natural asperities on fracture surfaces in creating tortuosity of the flow path as the fractures close with stress has been demonstrated in the laboratory. With use of a 3-D CFD finite-element fluid flow code/model we show the degree to which shear offset can change the fracture fluid flow behavior.

In order to understand the liquid hydrocarbon resource distribution and producibility in Western Canada, we first updated regional maps of organic maturation, established the distribution of the oil window aerially and stratigraphically, and correlated this data with produced gas wetness. We focused our detailed studies on the most important stratigraphic intervals, each of which was to comprise the thesis research of a graduate student.

As part of our investigation into the gas and liquid hydrocarbons in place in shales, we undertook a detailed study of the volume, rheology, and chemistry of fluids during flowback after hydraulic completion of Montney Formation wells. The major ions in the flowback water, and hence total dissolved solids (TDS), increase over the flowback period with rare exception. SO_4 concentrations are generally invariant. Physical mixing between the completion hydraulic fracturing fluid and the high TDS formation water in the fracture network, and through countercurrent imbibition, is the dominant process that is influencing the flowback water chemistry. In addition to physical mixing, other potential contributors to high TDS are ion diffusion and/or osmosis.

Cl^-, $\delta^{18}O$, and δ^2H were treated as conservative tracers to calculate the proportion of formation water contributing to flowback water. The initial (early time) flowback water samples are comprised of 10-35% formation water whereas in the final flowback, water samples (prior to putting the well on production) are 40-60% formation water. For the studied wells, the calculated volume of hydraulic fracturing fluid recovered based on the mixing proportions is typically < 10% of the injected fluid. For well constrained wells, we compared the time between end of completion and start of flowback (shut-in time/soak time) with cumulative hydrocarbon production at 30 days and two years. Our data is inclusive in showing if soaking is bad, good, or indifferent to production rate or cumulative production- if soaking is important, its effects, even in our well constrained data, is masked by a plethora of other variables.

Prospective Devonian shale reservoirs, the Horn River and Liard basins, Cordova Embayment, and adjacent western Alberta, were investigated using petroleum systems protocol ground-truthed with fluid analyses and petrophysical and geochemical analyses of core and cuttings. Due to the overmaturity of the strata in most of the study area, the Rock Eval S2 peaks are low or absent and hence Tmax, a common maturity index, is not reliable. Also, due to the age and depositional setting of the strata, vitirinte is rare. Regionally, the maturity of the Devonian shales increases from Alberta, where the strata are mature to the west and north where the strata are markedly overmature. Because of high thermal maturity, the liquid hydrocarbon potential of Devonian shales in the British Columbia portion of the study area is low, whereas in Alberta, due to shallower burial, the prospectivity is higher. Modeling representative wells from the studied basins shows that peak burial depth and temperature were reached during the Late Cretaceous and early Paleocene. However, the onset of oil generation varies by hundreds of millions of years over the spatial extent of the study area. In the Liard Basin, the Devonian shales have been generating oil since the Carboniferous, reaching peak oil generation (transformation ratio = 50%) in the early Triassic, whereas the onset of oil generation in the Alberta wells occurred at 100 Ma at the earliest (if oil generation occurred at all) and peak generation occurred during the Late Cretaceous. In nearly all of the well locations modelled in this study, the transformation ratio reached 100% during foreland subsidence, which results in the current dominantly dry-gas potential nature of the Devonian petroleum system.

One of the major objectives of our study was to investigate the influence of diagenesis and thermal maturity on the pore structure evolution of organic-rich, shale gas, and shale oil producing reservoir rocks. The Duvernay Formation is well suited for this study because the formation spans multiple thermal maturity boundaries from immature to overmature with increasing burial depth, and is generally compositionally similar over this range of maturities. A pore to basin scale study of the Duvernay Formation was thus undertaken with particular emphasis on determining how permeability of shales to liquids varies with shale diagenesis and lithofacies. Comparison of pore structures from samples of varying maturity provided insight into the impact of thermal maturity and compaction on mudrock microstructure and permeability. Organic-matter hosted, fine mesoporosity is visible with FE-SEM imaging from the onset of the oil window (HI = 348 mg HC/g TOC) and the development of organic matter-hosted pores increases in both size and abundance systematically with increasing maturity into the dry gas window. The pore size distribution, as measured by N_2 low pressure gas adsorption, shows a progressive increase in fine pore sizes with thermal maturity from the oil window through the dry gas window and the subsequent loss of larger pore modes. Macropore volumes are highest within the shallow, immature samples and progressively decrease with increasing maturity and burial due to compaction. Average helium pulse-decay permeability for samples from the wet gas and dry gas window are an order of magnitude higher than oil window samples. In general, this is a result of the development of fine pore sizes with maturity associated with organic matter. Within the wet gas window, permeability is dominantly controlled by the coarse meso- to macropore size fraction, which is associated with increased total quartz and feldspar content. The permeability for dry gas window samples is determined by a greater proportion of fine pore volumes correlated to relatively higher total clay, quartz, and feldspar content.

Regional mapping of lithofacies in the Duvernay was paired with reservoir characteristics including mineralogy, total porosity, organic matter (OM) content, net reservoir thickness, potential fracture barriers or baffles, reservoir quality impairments, and the impact of reef development. Wireline logs calibrated with laboratory measurements and artificial neural networks have enabled quantitative to semi-quantitative mapping of reservoir quality based mainly on mineralogy, TOC, and porosity.

Characterizing the Doig Formation through a petroleum system analysis approach was a major goal of this research proposal. The Doig Formation, although locally developed as a conventional reservoir, is considered a prospective unconventional target, which has largely been overlooked due to the greater prospectivity of the underlying Montney Formation. This study, which is still in progress, includes mapping the spatial distribution of lithofacies, total organic carbon content, organic matter quality, mineralogy, porosity, and permeability on a regional scale in northeastern British Columbia. Detailed wireline interpretations calibrated to core analyses have facilitated extrapolating facies, geochemistry, and geomechanical properties to non-cored areas. Petroleum system modeling will be used to reconstruct and determine the timing of thermogenic hydrocarbon generation, migration, expulsion, and retention.

Acknowledgments

The study was encouraged, catalysed and funded by Geoscience BC. We particularly thank Carlos Salas, VP of Geoscience BC, for his assistance and guidance in making the study possible. For this study, additional financial support was received from the Natural Science and Engineering Research Council and logistic and financial support was obtained from petroleum exploration and development companies and the petroleum service industry. In particular we acknowledge EnCana, Chevron Canada, Husky Oil, Trican Well Services, and Canadian Natural Resources for their generous financial support and intellectual contributions. Numerous other companies provided important logistic support to various components of sub-studies of this research program.

Introduction and Background

The rapid growth of the unconventional shale gas and shale oil industry has outpaced our understanding of the processes that determine gas and liquids in place as well as our methods for quantifying flow characteristics of the rocks, particularly when multiple phases are present. A three year research program was undertaken at The University of British Columbia with the overall goal of better understanding the occurrence of liquid hydrocarbons in shales and the factors that contribute to their producibility. The study was encouraged, catalysed and funded by Geoscience BC. For this study additional financial support was received from the Natural Science and Engineering Research Council and logistic and financial support was obtained from petroleum exploration and development companies and the petroleum service industry.

The study focused on British Columbia producing and prospective shales but also included analyses of other producing shales in Western Canada and the United States for comparative purposes.

Every aspect of the research involved the training of highly qualified personnel. The study is comprised of an interrelated series of research projects by graduate students, post-doctoral fellows and research associates at UBC which cumulatively addressed the overall objectives of the research. The legacies of the study are important contributions to the science and engineering of unconventional reservoirs and the better understanding of the liquid hydrocarbon resources in Western Canada and their producibility. Further accomplishment of the study are the successful training of highly qualified personnel, and the expansion of The University of British Columbia's unconventional resource laboratory to a world class facility.

In this report the salient observations, interpretations and conclusions are presented. This report provided an overview of the studies and conclusions For the detailed results of the studies the relevant thesis or published papers need to be consulted. Some of the research is still in preparation for publication and two thesis projects remain in progress. The completed research that comprises graduate student thesis are available for free download from The University of British Columbia library using the Uniform Resource Locators (URL) provided in the body of the report. Published papers are referenced in the text of this report and in the reference section of the report.

Results

The project as designed had two interrelated objectives: a) quantifying gas and liquid hydrocarbons in place and flow characteristics of shale gas and oil reservoirs; and b) quantifying gas in place and flow characteristics of fine-grained facies in Western Canada. The salient results of the study are summarised below.

a) Quantifying gas and liquid hydrocarbons in place and flow characteristics of shale gas and oil reservoirs

The methodologies currently used to characterize the pore systems, hydrocarbon storage capacity, and flow characteristics of the shale matrix are mainly a hybrid mixture of specialised methods used for coals and conventional reservoir rocks and have been applied to shales with limited consideration of their unique and varied properties or the physics of extremely small places.

Shales, in comparison to conventional petroleum reservoirs, are unique in their fine-grained nature and resulting nano- to micrometre scale pore systems. Characterising pore systems is important as they are the location of both storage and transport of hydrocarbons. The geometry of the pore systems and composition of the pore walls influence hydrocarbon production through capillarity and permeability, and by factors recently recognized, including pore size-dependent phase envelopes in nanometer scale pore and capillary condensation.

i. Insights into pore structure characterization and permeability measurement of fine-grained sedimentary reservoir rocks in the laboratory at reservoir stress states

The research by Eric Letham (PhD, 2017, https://open.library.ubc.ca/cIRcle/collections/ubctheses/24/items/1.0363004) has made a major contribution to understanding the pore structure and resulting flow characteristics of shale (refer to papers listed in contributions). The highlights of this research are summarised here.

Klinkenberg Gas Slippage Measurements as a Means for Shale Pore Structure Characterization

This investigation was undertaken because established techniques that have been successfully used to characterize pore systems in coarse-grained reservoir rocks lack the resolution and scalability required to adequately characterize the nano- to micrometer scale pore systems found in fine-grained rocks and cannot be applied on stressed samples.

Klinkenberg gas slippage measurements are a useful tool for analyzing the pore structure in shale in that they provide insight into the geometry of pores in stressed samples as well as show how pore structures will change with stress during production. Slippage measurements only characterize the effective porosity; however, this is desirable for evaluating flow and storage properties. Because slippage measurements are derived from permeability measurements, they are weighted to the portion of the effective porosity responsible for fluid flow. This characteristic allows comparison of the geometry of pores and pore throats responsible for flow parallel to bedding to those responsible for flow perpendicular to bedding, but limits the utility of slippage measurements for analyzing storage properties. Slippage measurements in conjunction with scanning electron microscopy, mercury injection capillary pressure analyses, and low pressure adsorption, collectively contribute to a more complete characterization of pore structures in shale.

Slippage analysis yields insight into the complex responses of these rocks to stress that other methods of pore structure analysis currently being employed to characterize shale pore systems are blind to. Slippage measurements on samples at a range of stress states revealed two orders of magnitude in slippage variation over a five order of magnitude permeability range. Slippage measurements are negatively correlated with permeability and follow similar trends to those found in other studies on higher permeability rocks. The results allow interpretation of the relative contribution of tortuosity and pore size to permeability anisotropy. Slippage, and therefore average effective pore size, was found to vary up to one order of magnitude at a given permeability, warranting investigation of the significance this might have on flow properties and ultimately hydrocarbon production from shale.

Quantitative Validation of Pore Structure Characterization Using Gas Slippage Measurements by Comparison with Predictions from Bundle of Capillaries Models

Characterizing pore structure geometry is fundamental to understanding and predicting many aspects of porous media behavior. Fully characterizing reservoir rock pore structure geometry is expensive and technically challenging due to the geometrical complexity and small length scale of these media, and it is impossible for low permeability reservoir rocks with pore structure length scales below the resolution limits of even the most advanced imaging techniques. We have investigated the quantitative validity of characterizing pore structure geometry using gas slippage measurements. Compared to other pore structure characterization techniques, such as mercury intrusion porosimetry and CO_2 and N_2 gas adsorption, the gas slippage technique has the advantageous attribute of being applicable to samples confined at in situ reservoir stress conditions. Using pore structure geometry characterizations determined at ambient surface stress conditions as inputs for subsurface reservoir models leads to inaccurate predictions of reservoir behavior. It is therefore desirable to use pore structure characterizations determined at subsurface reservoir stress conditions as model inputs.

In this study, we quantitatively validated the gas slippage technique, which is capable of pore geometry characterizations at in situ stress, by comparing pore sizes estimated from gas slippage measurements with pore sizes independently estimated using bundle of capillaries models. We find 99% of the gas slippage data result in pore size estimates that are consistent with bundle of capillaries models with geologically plausible inputs of porosity and tortuosity and broadly similar (though not identical) trends of pore sizes calculated from gas slippage measurements with the trends of pore sizes estimated using bundle of capillaries models using tortuosity and porosity. Conventional pore geometry characterization techniques, such as mercury intrusion porosimetry, CO_2 and N_2 adsorption, and scanning electron microscopy, are not cost effective methods for characterizing pore structure at in situ reservoir stress states, whereas gas slippage measurements is. The findings of this study are particularly significant for the successful exploitation of shale gas and shale oil reservoirs that are typically highly stress sensitive and, by definition, have small-scale pore structures.

The Impact of Gas Slippage on Permeability Effective Stress Laws: Implications for Predicting Permeability of Fine-Grained Lithologies

Quantifying permeability at reservoir stress and at the range of stress states that will be experienced during production from a reservoir is necessary for modelling and ultimately predicting fluid production. Accurate permeability prediction of fine-grained lithologies, such as shale oil and shale gas reservoirs, is especially important because permeability is more sensitive to stress in fine-grained lithologies than in the coarser-grained lithologies of conventional hydrocarbon reservoir rocks. Predicting permeability of fine-grained lithologies in the laboratory is complicated by their nano- to micrometre length-scale pore systems, which can result in significant departure from the Darcy flow regime due to gas slippage when a gaseous fluid flows through the rock. Laboratory measurements of permeability are commonly made at lower-than-in situ reservoir pore pressures, where gas slippage is more significant. In this study, we show, based on experimental data, the potential for errors introduced by not considering gas slippage in permeability predictions derived from laboratory measurements and show the impact of gas slippage on experimentally-derived permeability effective stress laws. Gas slippage drives apparent permeability effective stress law coefficients towards values less than one at lower pore pressures and at higher confining pressures. How much gas slippage contributes to flow-rate, and therefore increases apparent permeability, depends on the probing fluid used for permeability measurements, and the pore pressure range over which the permeability is measured, and the pore structure of the rock. The magnitude of permeability variation due to gas slippage in comparison to the stress sensitivity of permeability determines how significant the impact of gas slippage will be on experimentally-derived permeability effective stress laws. For fine-grained lithologies, the common assumption that gas slippage can be neglected at pore pressures higher than 7 MPa, when determining a permeability effective stress law using a gaseous probing fluid, needs to be abandoned, and previous studies utilizing this assumption need to be thoroughly re-examined.

Very few robust permeability effective stress laws for fine-grained sedimentary rocks have been published. Determining robust effective stress laws for more fine-grained samples will allow assessment of how likely it is that permeability-stress relationships determined assuming $\alpha = 1$ can be extrapolated to in situ reservoir pressure conditions from laboratory measurements made at lower-than-in situ pressure.

Multi-Phase Flow Phenomena in Fine-Grained Reservoir Rocks: Insights from Using Ethane Permeability Measurements over a Range of Pore Pressures

Hydrocarbons in shale oil and shale gas reservoirs travel in the presence of multiple immiscible fluids through small pores in the fine-grained matrix prior to reaching a fracture network leading to the wellbore. Immiscible phases include one or both of liquid and gaseous hydrocarbons as well as connate water and imbibed hydraulic fracturing fluid. Capillary pressures across the interfaces of these immiscible phases can be enormous due to the small size of pores in shales (nanometre to micrometre length scale). The small pore length scale also means that geometrical constrictions imposed by fluid adsorbed to pore walls can significantly inhibit flow; hence, effective permeability of hydrocarbon phases are very sensitive to the presence and saturation of the different fluid phases.

To date, researchers have had minimal success investigating multiphase flow characteristics of shale due to challenges associated with characterizing reservoir rocks with small length scale pore systems. These challenges include the difficulty in controlling and monitoring fluid saturations and distributions in intact samples and, because of their inherently low permeability, difficulty in quantifying the very low flow rates characteristic of shales. In this study, we investigated multiphase flow phenomena in fine-grained rocks by measuring effective permeability of a suite of shale samples to gaseous ethane over a range of pore pressures up to the saturated vapour pressure (3.59 MPa at 18 degrees Celsius). Saturation of liquid/semi liquid ethane increases with increasing pore pressure, due to adsorption and capillary condensation, resulting in decreases to ethane gas permeability that vary across a suite of samples with varying pore size. By measuring pore size of the sample suite using gas slippage measurements, we show that the largest drops in ethane relative permeability take place in rocks with the smallest pores. We show that gas slippage measurements can be used to predict relative permeability and therefore aid in predicting the deliverability of hydrocarbons from a shale oil or shale gas reservoir.

ii Importance of tortuosity and asperities on fracture permeability in shales.

The importance of tortuosity and asperities to flow and thus fracture conductivity is of particular importance to shales due to their low inherent permeability and compressibility. As either natural or induced fractures close with increasing stress during production, the rough walls (asperities) of the fractures create a progressively more tortuous flow path such that the predicted fracture permeability deviates markedly from that assumed for planar fractures. Post doctoral fellow, A. Hosseinian's research focused on developing relationships relating fracture permeability with fracture surface morphology, and changes to this with respect to shear displacements using a 3-D fluid flow Computational Fluid Dynamic (CFD) finite-element approach based on Montney Formation shale. Results using the 3-D CFD finite-element fluid flow code FLUENT show that fracture surface roughness controls the degree to which a small shear offset can significantly change the fracture fluid flow behavior. Pressure drops are calculated for fluid flow travelling along different directions (i.e. parallel and perpendicular) relative to mated and non-mated rock fracture surfaces (Figure 1). The results indicate the existence of fluid flow anisotropy along different directions through the rock fracture. Although much further research is needed, the studies to date provide an exciting foundation for both further laboratory tests and numerical modeling which should yield a closure stress- fracture conductivity model that can be used to predict changing conductivity (and thus producibility) with stress.

The variation of fracture conductivity of extension and shear fractures in shales of a variety of mineralogy and fabric is part of continuing research by MSc student Scott Hazel. Preliminary studies show that impact on conductivity of even minimal offset of shear fractures as compared to almost no conductivity along well mated extension fractures.

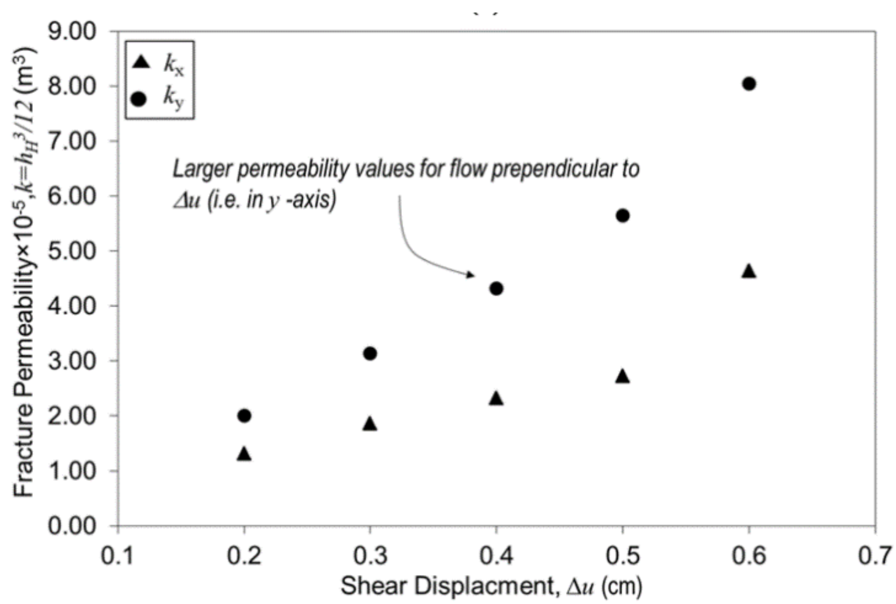

Figure 1. Variation in fracture permeability with direction and magnitude of shear displacement for a Montney shale (Hosseinian et al., 2015).

iii. Measuring liquid permeability, multiphase flow, and relative permeability in ultra tight rocks

In order to better understand multiphase flow and determine relative permeability in shales it was necessary to develop a methodology and equipment capable of measuring pulse decay and ultra low flow rates through permeability to a variety of fluids under reservoir conditions. To this end, Erik Munson (PhD, 2015, https://open.library.ubc.ca/cIRcle/collections/ubctheses/24/items/1.0166722) and others constructed a novel pulse decay liquid permeameter and developed suitable algorithms and associated code for analyses of the data. The legacy of this research, in addition to a great data set, is a well equipped laboratory and protocols for characterising flow properties of ultra low permeability rocks.

iv Controls and variability of the flowback water inorganic chemistry and rheology of the Montney Formation

As part of our investigation into the gas and liquid hydrocarbons in place in shales we undertook a detailed study of the volume, rheology, and chemistry of fluids during flowback after hydraulic completion of Montney Formation wells. Most of the results of this study comprise the MSc thesis of J. Owen (MSc 2017, https://open.library.ubc.ca/cIRcle/collections/ubctheses/24/items/1.0362574)) which is freely available at the URL provided. Much of the text below is extracted from the thesis and/or papers in preparation.

The Montney Formation is the most important unconventional shale reservoir in Canada and currently contributes about 30% of the total natural gas production in Canada. The flowback fluid provides a window into the reservoir and fracture system dynamics following completion. After hydraulic fracturing and before production, high salinity water flows from oil and gas wells for a period of time ranging from days to weeks. The salinity of the water increases over time and can be used to investigate processes that are occurring in the subsurface. The main influence on the chemistry of the flowback water is mixing between the injected fluid and the water in the formation and the amount of time that the injected fluid remains in contact with the rock.

In our study, flowback water from 31 wells located on 9 well pads (Figure 2) was sampled over time and analyzed for major ions, key minor ions, and $\delta^{18}O$ and $\delta^{2}H$ isotopes. The injected hydraulic fracturing fluids and produced waters, if available, were analyzed for the same parameters. The results of the study were then used to compare the flowback water chemistry between wells and investigate the variables that have a significant influence on the chemistry. The participating industry partners provided additional data such as details related to the drilling, completion, and flowback program. Additional reservoir data including mineralogy, petrophysics, and subsequent well performance was integrated into the study.

Montney Formation flowback water chemistry through mixing calculations and geochemical modelling

The major ion chemistry of the Montney flowback water provides insight into the geochemical processes that are occurring in the reservoir. The major ions in the flowback water, and hence total dissolved solids (TDS), increase over the flowback period with rare exception. SO_4 concentrations are generally invariant. There is variability in ion concentrations between wells. Wells completed at the same site and within the same stratigraphic interval generally show greater similarity in flowback water chemistry relative to those completed at different sites, which is interpreted to be due to the wells on the same site having comparable completion parameters and reservoir properties.

The makeup water for the completion fluid in the studied wells was mainly fresh water and hence the increasing major ion concentrations in the flowback water over the flowback period indicate that mixing between the relatively low TDS hydraulic fracturing fluid and the high TDS formation water is the dominant geochemical process that is influencing the flowback water chemistry. In addition to physical mixing between the injected fluid and formation water accessed in the fracture network and through countercurrent imbibition, other potential contributors to high TDS are ion diffusion and/or osmosis; however, it was not possible to differentiate between these processes and all may be adding to the increasing TDS.

Cl^-, $\delta^{18}O$, and δ^2H were treated as conservative tracers to calculate the proportion of formation water contributing to flowback water. The initial flowback water samples are comprised of 10-35% formation water whereas in the final flowback, water samples (prior to putting the well on production) are 40-60% formation water. Since there is a significant component of formation water in the fluid recovered during the flowback period, the amount of completion fluid recovered is much less than the volume of total fluid recovered. For the studied wells, the calculated volume of hydraulic fracturing fluid recovered based on the mixing proportions is typically < 10% of the injected fluid.

The proportion of formation water recovered in the flowback water is impacted by numerous definable factors and some factors that remain elusive. A multiple regression analysis identified shut-in time as an important variable, with longer shut-in correlating to higher concentrations. The chemistry of hydraulic fracturing fluids and formation waters were found to be important variables for some ions. The low correlation between the proportion of formation water in the flowback water and the length of the flowback period indicates that many variables are influencing mixing, including the length of the shut-in period and the extent and complexity of the fracture system. Using our three tracers provided a method to check the results through a comparison of the three mixing ratios obtained allowing for a representative range in ratios to be determined for each flowback water sample. In the site B, site E, and site F wells, the comparison between the mixing ratios calculated with the three tracers indicated that some of the isotopic results were contaminated. In well H-1, the use of multiple tracers allowed for the identification of potential mixing with a third fluid source with a different geochemical signature, in addition to the hydraulic fracturing fluid and the formation water. Potential fluid sources, in addition to the injected fluid and the formation water, include high permeability lenses and contiguous formations.

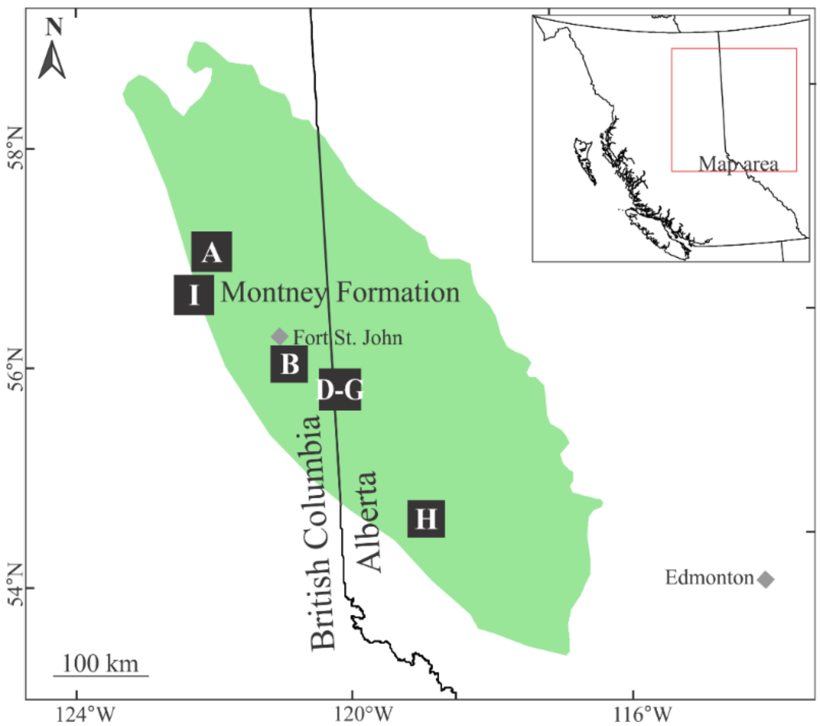

Figure 2. Location of the 8 study sites (A, B, and D-I). Wells completed in the upper Montney Formation are located at site A (8 wells), site B (2 wells), site D (2 wells), and site H (1 well). Middle Montney Formation wells are located at site D (2 wells), site E (4 wells), site F (2 well), and site G (1 well). The two wells located at site I were completed in the lower Montney Formation.

We subsequently used geochemical modelling to determine what processes, other than mixing, account for flowback water major ion chemistry. We find Na and K concentrations in the flowback water can be explained by mixing for the vast majority of the study wells, whereas the Ca, Mg, and Sr concentrations are influenced by a combination of mixing and ion exchange. Ion exchange causes the concentrations of the divalent ions to be lower over the course of the flowback period, relative to if only mixing was occurring. The Ca concentrations in flowback water are minimally impacted by calcite precipitation; the majority of wells do not show any evidence that calcite is precipitating in the formation, even though the mixed fluids are generally saturated with respect to calcite. The geochemical models for flowback water in wells A-2, A-3, A-6, D-1, D-2, D-3, the site E wells, the site F wells, and well H-1 are undersaturated with calcite and hence the potential for calcite dissolution exists when the hydraulic fracturing fluid is injected into the formation and the proportion of formation water in the mixed fluid is low.

SO_4 concentrations is not accurately modelled by mixing and are often higher than the values predicted in the mixing models. The elevated SO_4 concentrations may be related to the oxidation of pyrite or H_2S due to the injection of the hydraulic fracturing fluid as proposed in other studies. The decreasing SO_4 concentrations seen in the flowback water from the site I wells may be related to SO_4 reduction by bacteria.

Important minor ions included in the study are Ba, B, and Li. Ba concentrations are likely related to barite dissolution/precipitation and are highest where sulfate concentrations are low. B and Li concentrations are both dominantly influenced by mixing and may vary due to differences in formation water chemistry.

As part of our study, we compared the time between end of completion and start of flowback (shut-in time and also referred to as soak time) with cumulative production at 30 days and two years (Figure 3). We also included in our comparison the amount of completion fluid pumped per meter completed. In this comparison we attempted to only include wells with a minimum of operational issues during completion and flowback. In the literature there have been strong arguments made for the both the benefits and deleterious impacts on production of protracted soaking wells We consider the data presented in our study to be inclusive in showing if soaking is bad, good, or indifferent to production rate or cumulative production.

Overall, the results contribute to the growing knowledge on flowback water chemistry and its use in investigating the processes occurring in the reservoir during hydraulic fracturing.

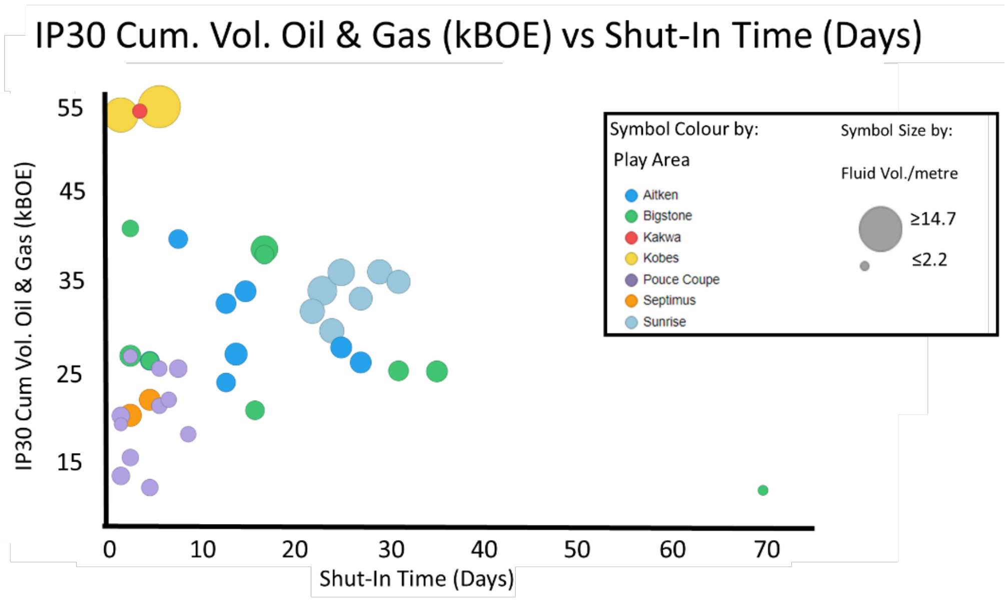

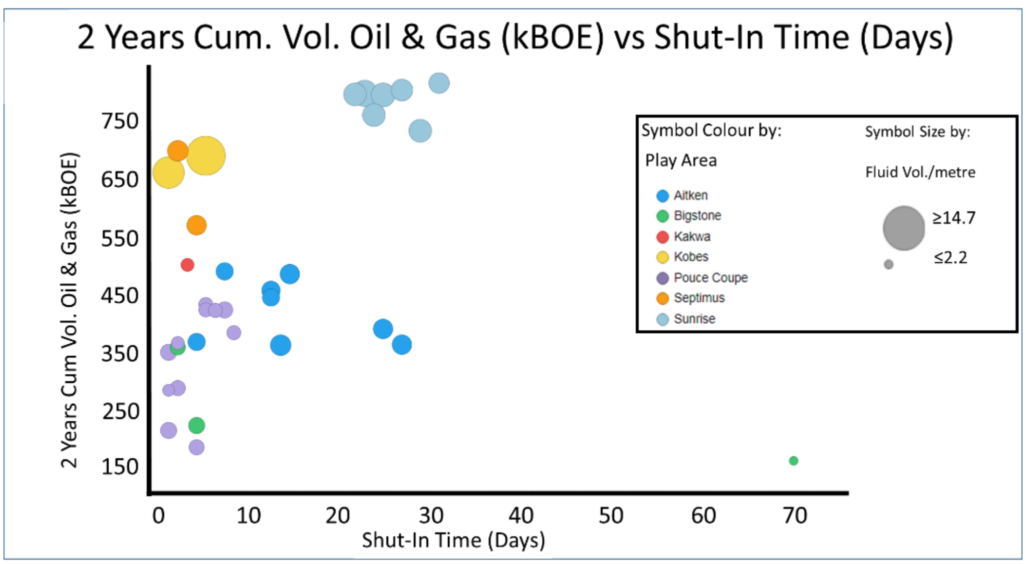

Figure 3. Cross plot of cumulative production at 30 days and 2 years vs shut-in time (time between end of completion and start of flow back)

Stratigraphic and Areal Variation in Flowback water chemistry of the Montney Formation

A myriad of variables related to reservoir properties, completion design, and response of the reservoir to completion impact the volume and chemistry of the flowback water and subsequently reservoir production. In order to understand the importance of these variables and subsequent impacts on production, we investigated Montney flowback liquids in wells across northeastern British Columbia (Figure 2) and in wells completed at different stratigraphic levels in the Montney.

The concentrations of the major ions increase over the flowback period for all wells studied; however, the rate of increase varies between different sites and sometimes between wells on the same drilling pad. The rate of change for major ion concentrations during flowback is due to the degree/rate of mixing between the relatively low TDS hydraulic fracturing fluid and the high TDS formation water. There are several potential variables affecting the rate of increase at different sites. Trend analysis provides a method for grouping the wells based on the increase in the major ion concentrations over flowback time. The majority of the major ions fall within the following groups: slow rate of increase – sites E-G, well I-1, site A (Cl, Sr); moderate rate of increase – sites B-D, well I-2, site A (TDS, Na, K); and rapid rate of increase – site H, site A (Ca). One of the few consistent areal trends in flowback water chemistry is the increasing Sr concentrations from southeast to northwest in wells completed in the upper Montney Formation.

Of the variables considered in the current study, those identified as important to the flowback water chemistry were the shut-in time, the hydraulic fracturing fluid chemistry (Cl, Ca, Mg, Sr – for the initial flowback), and the formation water chemistry (TDS, Cl, Ca, Mg – for the intermediate to late flowback; tables 1 and 2). Using the last sample flowback water chemistry to approximate the formation water chemistry shows that the shut-in time decreases in importance over the flowback period, while the relative importance of the last sample flowback water chemistry, as a proxy for formation water, increases. The positive correlation observed between the Ca and Mg concentrations in flowback water and the percentage of carbonates in the formation is not interpreted to be due to carbonate dissolution as the other major ions (e.g., Na) are also positively correlated with percent carbonate. The ratios of the monovalent and divalent cations to Cl show opposing trends with the percentage of clay. The monovalent cation ratio shows a positive correlation while the divalent ratio shows a negative correlation. This result indicates that cation exchange is occurring and increasing in importance with higher proportions of clay.

Table 1. Correlation coefficient (R^2) values for the initial sample flowback water chemistry and the variables of interest. R^2 values greater than 0.2 are in bold italic text, values greater than 0.5 are shaded in grey. Negative correlations are denoted by (-)

Parameter	**TDS**	**Cl**	**Na**	**Ca**	**Mg**	**Sr**	**K**
HF fluid chemistry	***0.31***	***0.42***	0.08	***0.32***	***0.34***	***0.53***	0.04
HF fluid volume per stage	0.09	0.10	0.05	0.08	0.11	0.15	0.08
Shut-in time	***0.59***	***0.55***	***0.59***	***0.57***	***0.47***	***0.55***	***0.69***
Number of stages	0.10	0.08	0.18	0.07	0.00	0.01	0.12
Breakdown pressure	***0.41***	***0.37***	***0.50***	***0.31***	0.17	***0.24***	***0.42***
Formation water chemistry	0.11	0.03	0.01	0.00	0.00	***0.21***	***0.55 (-)***
Chemistry of last flowback sample	***0.26***	***0.25***	***0.21***	***0.48***	***0.23***	***0.67***	***0.38***
Median carbonate	***0.47***	***0.47***	***0.34***	***0.53***	***0.67***	***0.57***	***0.52***
Median clay	***0.37 (-)***	***0.34 (-)***	***0.35 (-)***	***0.36 (-)***	***0.43 (-)***	***0.37 (-)***	***0.50 (-)***
Median feldspar	<0.01 (-)	<0.01 (-)	0.01 (-)	<0.01 (-)	0.01	0.01	<0.01 (-)
Median quartz	0.05 (-)	0.05 (-)	0.02 (-)	0.12 (-)	***0.20 (-)***	0.16 (-)	0.05 (-)

Table 2. Correlation coefficient (R^2) values for the intermediate-late flowback water chemistry and the variables. R^2 values greater than 0.2 are in bold italic text, values greater than 0.5 are shaded in grey. Negative correlations are denoted by (-).

Parameter	**TDS**	**Cl**	**Na**	**Ca**	**Mg**	**Sr**	**K**
HF fluid chemistry	***0.20***	***0.20***	0.14	***0.47***	***0.31***	***0.55***	0.02
HF fluid volume per stage	<0.01	<0.01	<0.01	<0.01	<0.01	0.06	<0.01
Shut-in time	***0.41***	***0.43***	***0.29***	***0.39***	***0.24***	***0.56***	***0.38***
Number of stages	0.13	0.10	***0.21***	0.08	0.02	0.04	0.16
Breakdown pressure	***0.29***	***0.27***	***0.32***	***0.21***	0.14	***0.34***	***0.38***
Formation water chemistry	***0.30***	0.09	0.05	0.05	0.09	0.14	***0.21 (-)***
Chemistry of last flowback sample	***0.44***	***0.38***	***0.57***	***0.66***	***0.64***	***0.68***	***0.70***
Median carbonate	***0.36***	***0.41***	0.17	***0.48***	***0.57***	***0.57***	***0.32***
Median clay	***0.35(-)***	***0.35(-)***	***0.25 (-)***	***0.32 (-)***	***0.44 (-)***	***0.39 (-)***	***0.45 (-)***
Median feldspar	<0.01 (-)	<0.01	<0.01	<0.01	0.03	0.01	<0.01
Median quartz	0.03 (-)	0.04 (-)	<0.01	0.12 (-)	0.12 (-)	0.16 (-)	<0.01

v. Retained liquids in place in shale and other fine-grained facies- impact of imbibition of oil based mud on core based oil saturations

Developing a predictive model for liquid production from shales, which is a goal of the study, requires an in depth understanding of the total petroleum system in northeastern British Columbia. The petroleum system of self-sourced shale reservoirs is complex. Hydrocarbons that are generated depend on kerogen type and thermal history, and hydrocarbons that are retained in shales are a fractionated part of the generated hydrocarbons. Retained hydrocarbons are also subject to alteration with additional burial and possibly further selective migration of secondary generated hydrocarbons. During production, the retained hydrocarbons are further fractionated such that the produced product does not necessarily correspond to that retained in the reservoir. Yet a further complication is the high capillary pressure, which is largely responsible for selective migration, retention, and production, and varies with pore structure and wettability, which in turn depends on mineralogy, fabric, fluids, and thermal history.

Prior to this study, it was common industry practice to measure oil saturation on shale core and to subsequently calibrate wire logs to this data in order to establish hydrocarbon liquids in place. As part of this research program it was necessary to determine the utility of measuring oil saturations in cores taken from shales drilled and cored with oil based muds (invert), which is the norm in the Montney and Duvernay Formations. Our concern was founded on our earlier studies that had established that the Montney Formation and much of the Duvernay Formation had mixed wettability and readily imbibed invert. We secondly wished to establish the utility of using historical Rock Eval type data (Esptialié, 1986) as either a direct measure or as an index for mapping retained hydrocarbons in the shales. Many thousands of Rock Eval type measurements exist for strata in western Canada from petroleum source rock studies and this data could provide a wealth of information for our study if shown to be reliable.

.

In order to test for possible core contamination by invert and to calibrate archived data, we undertook a study of Montney cores preserved at the well site. Eight millimetre diameter mini-plugs were cored perpendicular to the core axis in nitrogen from preserved whole cores in order to assess the effect of drilling fluid infiltration on hydrocarbon distribution and wettability. The plugs were taken a minimum of one half the diameter of the core from the base ends of the sample (Figure 4). This ensured that infiltration of drilling fluid from ends of the core sample did not influence results. Plugs were then sectioned into four or five, 1.1 cm pieces and designated Zones 1 through 4 (or 5), where Zone 1 is nearest the surface and Zone 4 represents the center of the core (Figure 4).

Our results for all cores from shales in the oil window through to the dry gas window cored with oil based mud show trends in the Rock Eval S1 peak (measured in mgHC/gram rock) and hydrocarbons from chromatography, from high values on the core margins to lower values at the center of the core. Such a trend, supported with more detailed geochemistry (Bustin et al., 2015), indicate sever contamination by invert, which extends for some cores through to core axis (Figure 5). These results clearly illustrate that care must be taken when selecting samples for mapping retained hydrocarbons and that the oil saturation calculations as routinely performed by commercial laboratories, even on preserved cores, must be viewed with extreme caution. The variation in wettability (contact angles) to oil, measured on new core surfaces perpendicular to the core axis do not show a significant trend with degree of invasion/imbibition of drilling oil. Such results probably reflect the dominance of new mineral surfaces created during sample preparation and the relatively small pore volume of the samples.

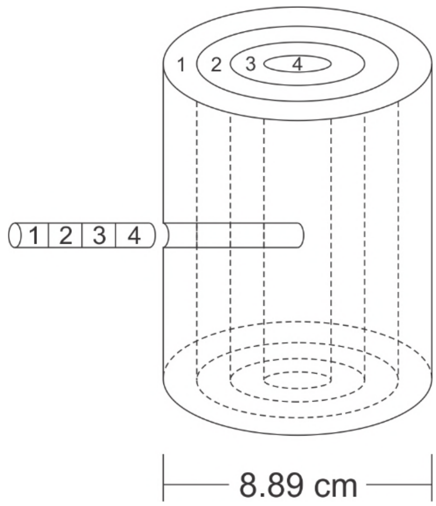

Figure **4** Sampling protocol: a mini- core about 8 mm in diameter is drilled from the outer edge of the core using nitrogen and subsequently sub-sampled into five sub-samples, labelled surface and 1 through 4.

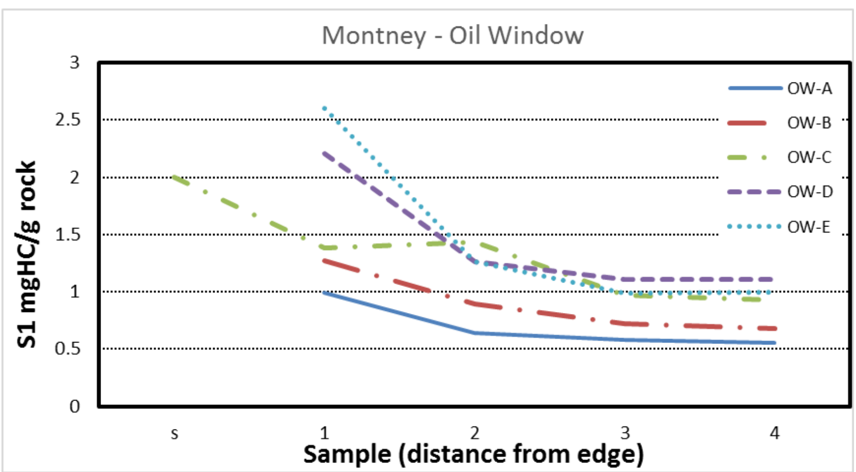

Figure 5. Examples of the Variation in S1 peak data (mgHC/gram rock) from Rock Eval type analyses from the face of the core to the centre for 5 samples (see figure for sample location).

b) Gas in place and flow characteristics of fine-grained facies in Western Canada.

In order to understand the liquid hydrocarbon resource distribution and producibility, we first updated regional maps of organic maturation and distribution of the oil window aerially and stratigraphically, and produced gas wetness. We focused our detailed studies on four of the most important stratigraphic intervals, each of which was to comprise the thesis research of a graduate student with cooperation of research associates. Although each study is unique, they share an overall research plan that is centred on integrating petroleum system analysis (PSA) to assist in predicting the distribution of producible hydrocarbons and favorable reservoir properties for production from unconventional reservoir rocks. Specifically, the goals of these studies were to determine the geological factors controlling the distribution of potentially producible wet gas, condensate, and oil. The research is multi-faceted and uses PSA ground-truthed with fluid analysis and petrophysical and geochemical analyses of core and cuttings to predict the types and volumes of generated and retained hydrocarbons. Key elements of each study were: 1) source rock evaluation: through quantification and mapping of the source rock properties across the basin, such as thermal maturity, kerogen type, kerogen abundance, and kinetic factors; 2) reservoir characterisation including storage capacity, producibility, response to hydraulic stimulation, capillary pressure, and wettability; and 3) 3-D basin modeling to resolve the timing of hydrocarbon generation, migration and retention, and reservoir development.

Below we describe some of the salient conclusions of our research to date.

i. Regional Variation in Organic Maturation and Gas Composition

Over the last forty years, a large volume of data has been collected on petroleum source rocks in Western Canada by government laboratories, university researchers, and industry. The retained (non-migrated) hydrocarbons in petroleum source rocks are now being exploited by horizontal drilling and fracturing as unconventional petroleum reservoirs. Much of the data collected for petroleum source-rock evaluation has new relevance for predicting the distribution and producibility of retained hydrocarbons referred to as shale gas and shale oil. As part of this study on predicting the distribution and producibility of liquid-bearing, fine-grained unconventional rocks (shales), new, publicly available data on maturity, source-rock properties, and production were compiled and integrated with EXbase[1] data to map and predict the liquids-production potential of source rocks. The gaps in the datasets were filled in by data from additional sampling and analyses detailed in the studies summarised in later sections of this report.

The present study of regional maturation builds on many excellent, previous studies and data compilations on source rocks in the Western Canadian Sedimentary Basin (WCSB). The variation in organic maturation and other source-rock properties in the WCSB occurs at multiple scales. The degree of organic maturation that governs hydrocarbon generation has been shown to occur at least at three scales, referred to as 1st, 2nd, and 3rd order variations by Bustin (1991, 1999). First-order variations that encompass the northeastern (Interior Plains) to southwestern

[1] [1]EXbase is a proprietary historical database of mainly geochemical data.

(disturbed belt) region show an increase in organic maturity for all strata. This is a reflection of the overall westward thickening of the sedimentary prism, and hence depth of current and paleo burial. Third-order variations are local highs and lows (bull's eyes on maturity maps) thought to be due to faulting (in the disturbed belt), thermal anomalies and, in some areas, likely a lack of control. The most important and well-established 2nd order variations in maturity occurs in the Peace River Arch of northeastern British Columbia and adjacent parts of Alberta. In this area, it was documented early on (Karst and White, 1980) that there is a reversal in thermal maturity (coal rank) from the southwesterly trends of increasing maturity (1st order variation in maturity) to one of southwesterly decreasing maturity in northeastern British Columbia and adjacent parts of Alberta. The importance of the reversal to oil exploration is that part of the WCSB succession in the deformed belt of northeastern British Columbia is within the oil window rather than being overmature with respect to the oil window, and thus is prospective for liquid-hydrocarbon exploration.

We have updated mapping of the regional variation in organic maturity in northeastern British Columbia and adjacent parts of Alberta. The results have been detailed in Bustin and Bustin (2016). The maturation data of surface exposures (Figure 6) for all analyzed horizons is generally consistent with northeastward-dipping isomaturity surfaces from the Interior Plains to the edge of the deformed belt, which mimics the current regional structure. Within the southwestern part of the study area, in the deformed belt, the isomaturity surfaces reverse and dip to the southwest and, where adequate data is available to allow validation, reverse once again to dip to the northeast. Superimposed on these regional trends are local highs and lows in maturity that define more complex patterns. Example isomaturity maps are presented here for select horizons only: Portlandian and Neocomian strata and the Upper Jurassic Gordondale Member (formerly the informal Nordegg member) of the Fernie Formation.

The maturation trends of Albian (not shown) as well as Portlandian and Neocomian strata (Figure 7) are similar, with the exception that the older strata have somewhat higher reflectance values (thermal maturity). Overall, on a regional scale, isoreflectance lines for both sequences parallel structural contours, which in turn parallel the northwest trend of the deformed belt. From northeast to southwest, maturation increases to a maximum value at the eastern edge of the deformed belt, then decreases and, where adequate data exists to allow validation (for example in NTS 93P and 93O), increases once again. To the northwest, maturation also decreases, but not as markedly as the trends noted in the southwest. Superimposed on these regional trends are low-maturation lows and highs that form 'bull's eyes' on the isomaturation maps.

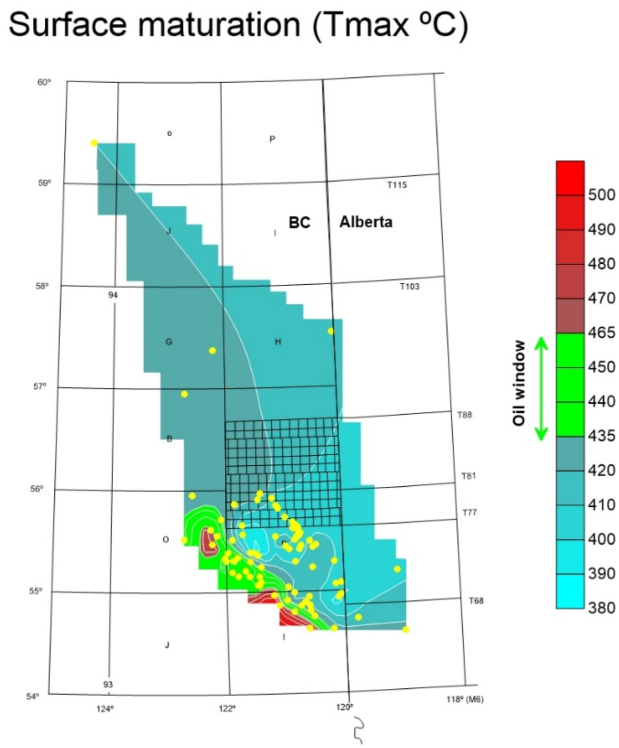

Figure 6. Isomaturity map of surface exposures, in the northeastern British Columbia portion of the Western Canada Sedimentary Basin. Only area up to edge of the deformed belt shown.

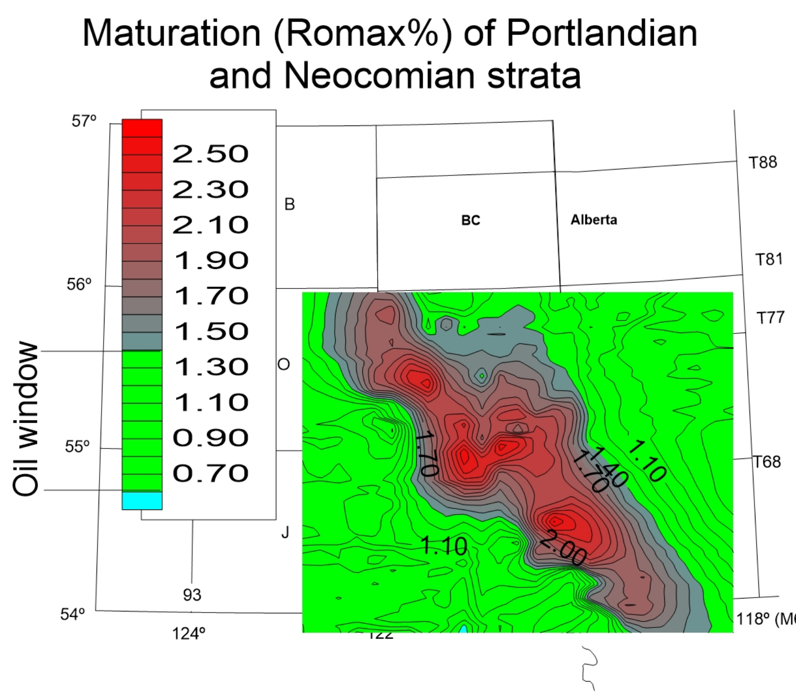

Figure 7. Isomaturity map for Portlandian and Neocomian strata in northeastern British Columbia. Contours are in % Ro_{max} from vitrinite reflectance.

Regional trends in maturation for the Lower Jurassic Gordondale Member of the Fernie Formation (Figure 8) and other intervals (not shown) were based on T_{max} values from Rock-Eval–type analyses and corroborated by reflectance data collected from adjacent carbonaceous strata. In general, the maturation trends for both the Gordondale Member and Shaftesbury Formation (not shown) mimic those of the Albian as well as the Portlandian and Neocomian strata: isomaturation lines parallel structural contours, as well as the edge of the deformed belt, and the maturity initially increases toward the southwest, then declines. The trend is similar for the Gordondale Member. However, where data are available to allow validation, a second increase in maturity is evident.

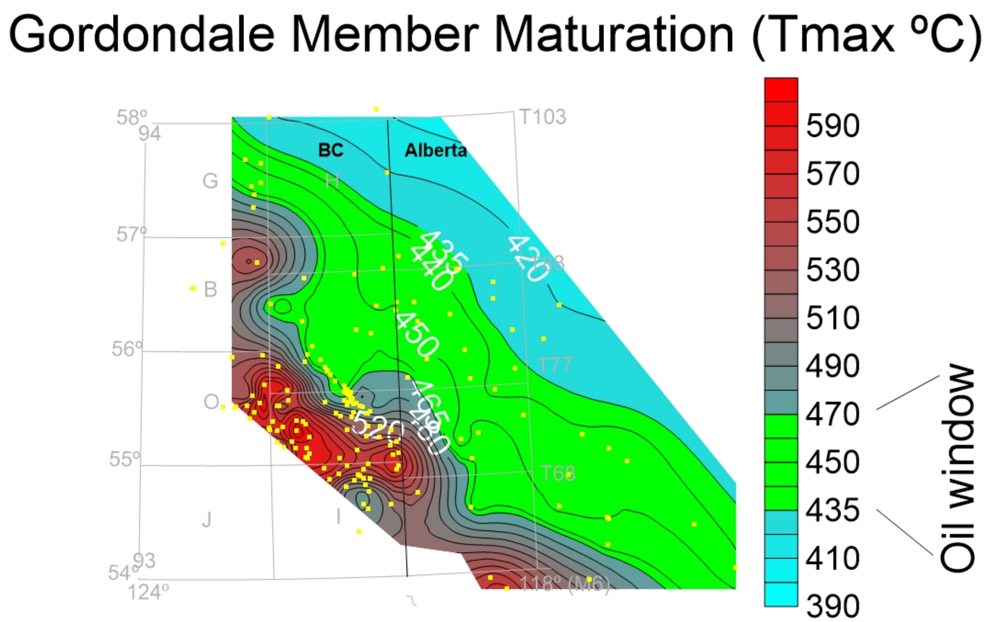

Figure 8. Isomaturity map for the Gordondale Member, in northeastern British Columbia, based on T_{max}ºC data and corroborated by some vitrinite reflectance data

Based on the combination of vitrinite reflectance and T_{max} data, the depth to the top (Ro = 1.35%; T_{max} 465ºC) and base (Ro = 0.65%; T_{max} 435º C) of the oil window, as well as the thickness of strata within the oil window, have been mapped throughout the study area (Figure 9a, b, c). The depth to both the top and base of the oil window decreases to the southwest from the Interior Plains, toward the eastern edge of the deformed belt, and then increases in the deformed belt. This trend mimics the patterns shown on isomaturation maps of selected horizons outlined above. In the southeastern and northwestern parts of the study area, the top of the oil window occurs at depths ranging up to 1400 m (subsea), whereas to the southwest, the top of the oil window is missing (projected to be greater than 2600 m above sea level). The base of the oil window occurs at depths ranging up to 3500 m (subsea) in the southeastern part of the study area, is eroded in the southwestern part of the study area (projected to depth, thus about 1500 m above sea level), and initially decreases and then increases in depth toward the northwest. The thickness of strata within the oil window varies from 200 to >2000 m (Figure 9c), with the thickest strata in the oil window occurring in the southeastern and northwestern parts of the study area.

A. Depth to base of oil window (subsea)

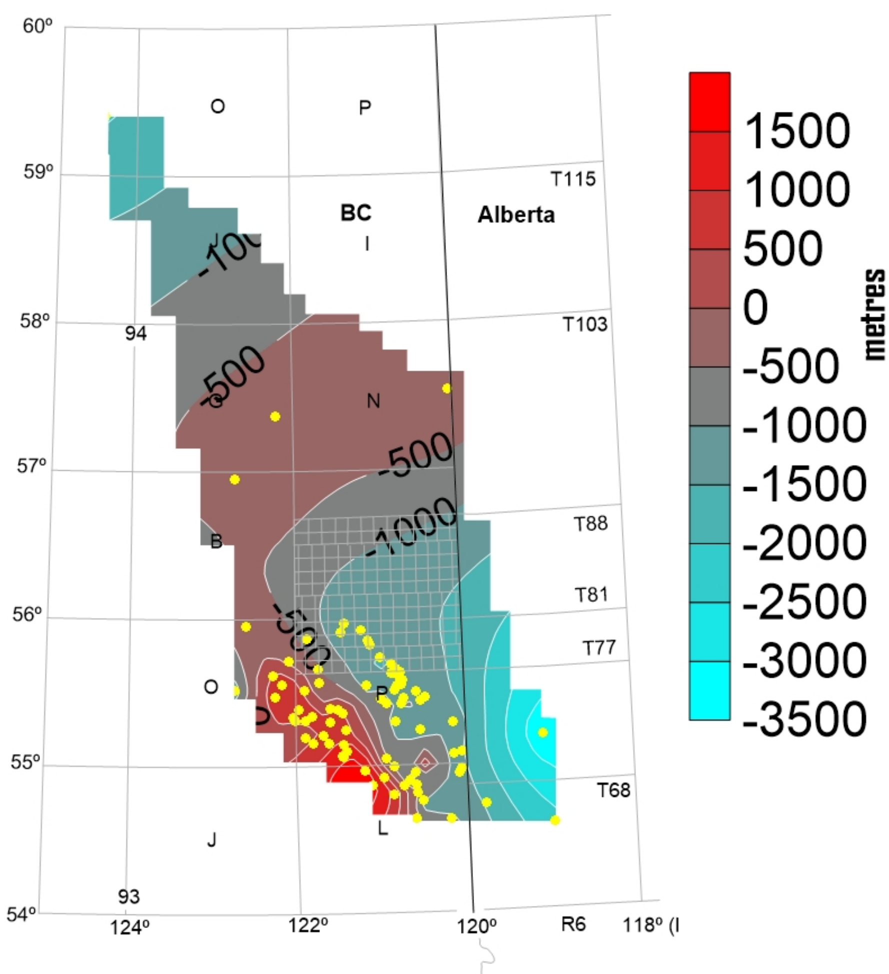

B. Depth to top of oil window (subsea)

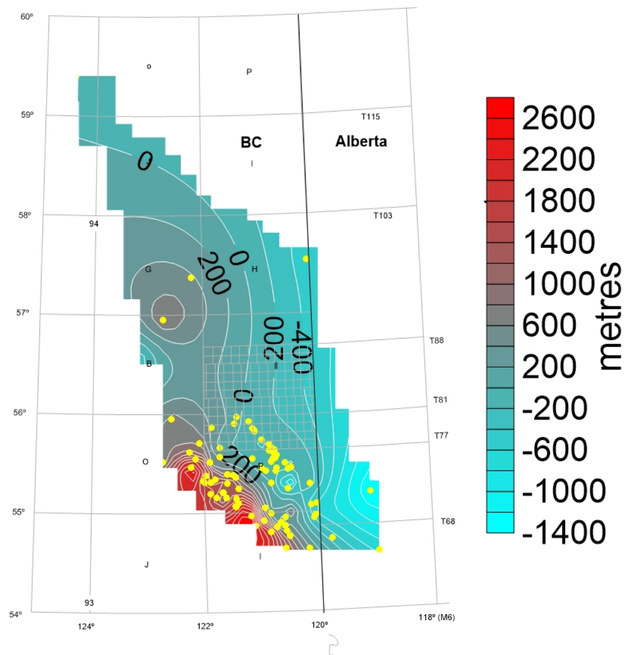

C. Thickness of strata in oil window

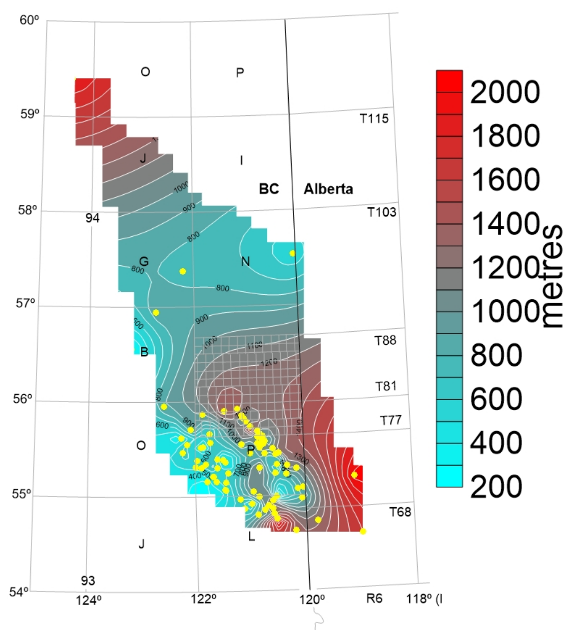

Figure 9. Regional maps, showing a) depth (subsea) to the top of the oil window; b) depth to the base of the oil window; and c) thickness for strata within the oil window in northeastern British Columbia. These maps are based on the assumption that the oil window is invariant with kerogen type. Horizon-specific data needs to include consideration of kerogen type.

As a result of the economic importance of the Montney Formation, a large number of wells cored in the formation have been tested over the last decade. Based on the integration of new data from this work, the thermal maturity of the Montney Formation is shown in Figure 10. Overall, maturity increases with depth of burial, but there is substantial variation that is at least partly attributable to varying paleogeothermal gradients, as determined from maturation gradients of individual wells (Bustin, 1991, 1999). The wetness of produced gas, as calculated from production tests (publicly available data), is mapped in Figure 11. On a regional scale, the degree of correlation between the variation in wetness and thermal maturity is as anticipated, with wetness initially increasing from northeast to southwest into the oil window and then decreasing at higher levels of maturity.

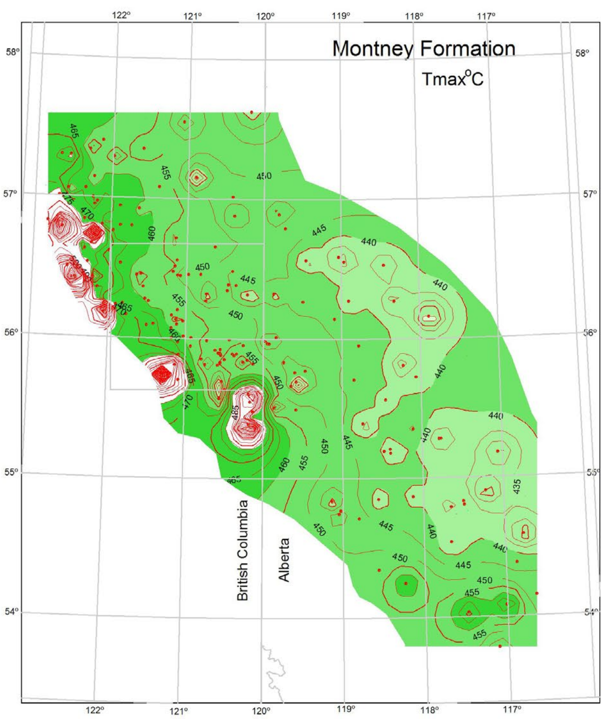

Figure 10. Regional thermal maturity of the Montney Formation, northeastern British Columbia, based on selective T_{max} values from Rock-Eval–type analyses. The lighter green corresponds to the early stage of the oil window and the darker green, to the last stage.

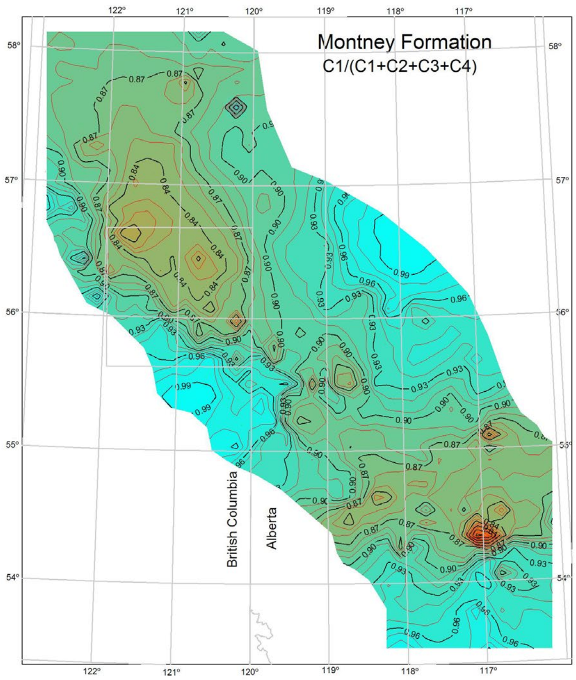

Figure 11. Gas wetness calculated using C1/(C1+C2+C3+C4), applied to gas hydrocarbons C1 through C4 (C1, methane; C2, ethane; C3, propane; C4, butane). The values are from analyses of samples collected in producing or tested wells in northeastern British Columbia.

ii Petroleum system analyses of Upper Devonian organic rich shales of the Horn River and Liard Basins, Cordova Embayment, and adjacent parts of the Western Canadian Sedimentary Basin

A multi-faceted study using petroleum systems analyses ground-truthed with fluid analyses and petrophysical and geochemical analyses of core and cuttings was undertaken to aid in prediction of hydrocarbon distribution, reservoir quality, and producibility of important Devonian shales. The study area encompasses the Horn River and Liard basins, Cordova Embayment, and adjacent western Alberta. This study comprises the MSc thesis (in progress) of T. Wilson and the following text is mainly modified from Wilson and Bustin (2019).

Due to the large geographic study area and paucity of core, the study focuses on wells along two NW-SE cross-sections such that the lateral variation in petrophysical properties and thermal maturity could be investigated with the southwestward increase in depth burial (Figure 12).

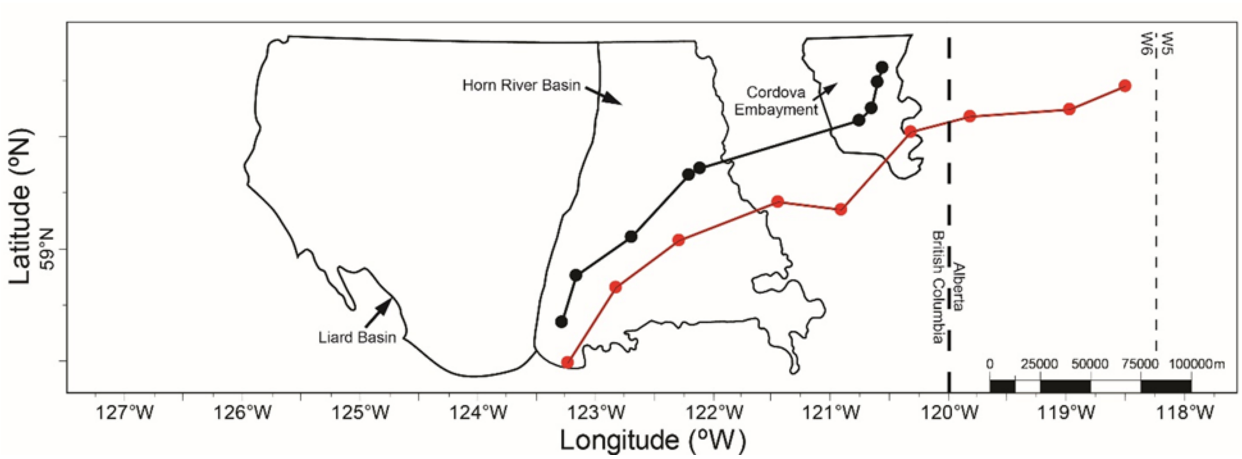

Figure 12. Well locations for which most analyses and modeling were performed.

The thermal maturity of the Devonian shales in the study area is difficult to map in detail. Due to the overmaturity of the strata in most of the study area, the Rock Eval S2 peaks are low or absent and hence Tmax, a common maturity index, is not reliable. Also, due to the age and depositional setting of the strata, vitirinte is rare. Regionally, the maturity of the Devonian shales increases from Alberta, where the strata are mature to the west and north where the strata are markedly overmature. In British Columbia, vitrinite reflectance measurements range from 1.75 to 3.2 %Ro with maturity generally increasing to the north and northwest across the Cordova Embayment, Presqu'ile barrier and Horn River Basin. Based on the limited available data, thermal maturity west of the Bovie Fault, are similar to in the Horn River Basin (2.6 to 3.1 %Ro) east of the fault, even though east of the fault, Devonian strata are approximately 1500 m deeper. Taken at face value these data suggest that peak maturity of the Devonian strata across northeastern British Columba predates the Late Cretaceous and Tertiary displacement along the Bovie fault (Maclean and Morrow, 2004).

Because of high thermal maturity, the liquid hydrocarbon potential of shales in the British Columbia portion of the study area is low. In tested Horn River Basin wells, gas wetness, as calculated according to Unrau and Nagel (2012), is less than 0.4, which classifies as dry gas. In the southeast corner of 094-I block, condensate has been reported for wells tested from Devonian shale and condensate produced from the overlying Jean Marie Formation is undoubtedly sourced from the underlying Muskwa Formation (Ferri and Griffiths, 2014).

Preliminary basin history plots based on examples from the Liard and Horn River Basins, Cordova Embayment, and western Alberta are shown in figures 13, 14, and 15. Full discussion of the models and sensitivity analyses of key variables are provided by Wilson and Bustin (2019).

The Nexen Beaver D-064-K well, located in the northcentral part of the Liard Basin, near the deformation front, was modeled using a present-day heat-flow value of 67 mW/m^2. The burial history of the Upper Paleozoic comprises several kilometres of sediment due to the thicknesses of the Besa River, Golata, and Mattson Formations. The organic rich Evie and Muskwa members within the Besa River Formation were buried to depths of 3225 m and 3110 m, with corresponding temperatures of 101º and 105°C respectively, by the end of Mattson Formation deposition (Figure 13). These depths were obtained by back stripping the model to Carboniferous/Permian time. This model entered the oil window (0.60% Ro) by 310 Ma. Throughout the Permian to Jurassic, the Fantasque and Toad Formations were deposited, along with multiple hiatus/non depositional periods. Thermal maturity was fairly constant throughout this time, reaching 0.90% Ro by Late Jurassic. During foreland subsidence, the Evie and Muskwa horizons reached maximum burial depths of 5375 and 5260 m, and maximum temperatures of 238 and 234°C, respectively. During foreland subsidence, thermal maturation increased from 0.9% Ro (oil window) to 3.3% Ro (overmature). By Late Cretaceous, all of the formations had reached thermal maturity levels necessary for hydrocarbon generation, with the majority of strata within the gas window or overmature. The erosion thickness for this model is 2250 m, corresponding to an erosion rate of 85m/m.y. Present-day maturities range from 1.7% Ro in the Mattson Formation to 3.4% Ro in the Muskwa member (Figure 13).

The Horn River Basin model for the Direct Gunnel C-095-L well, which is located in the southeastern portion of the basin, utilised a present-day heat flow of 88 mW/m^2. The Muskwa Formation was buried to a depth of 2025 m and a temperature of 83°C by Late Carboniferous, beneath the thick accumulation of the Fort Simpson and Mattson Formations (Figure 14). The Mattson Formation was subsequently eroded due to movement along the Bovie fault, as were the Toad and Fantasque Formations (Maclean and Morrow, 2004). Hydrocarbon generation began in the Lower Jurassic from the Muskwa Formation. A maximum burial depth of 3035 m and a temperature of 195°C, were reached during foreland subsidence. Thermal maturity for the Muskwa Formation increased from 0.6 (early-oil window) to 2.0% Ro (wet-gas window) during this time. The amount of erosion for this model is 1565 m, with an erosion rate of 52 m/m.y.

Present-day maturities range from 1.4% Ro in the Exshaw Formation to 2.6% Ro in the Klua Formation (Figure 14). The Direct Gunnel C-095-L model in the Horn River Basin calculates the onset of oil generation at 200 Ma for the Muskwa Formation. Thermal maturity values for the Muskwa Formation stayed near 0.6% Ro until the beginning of Cretaceous foreland subsidence when calculated maturity values increased to 2.0% Ro for this model. By the end of foreland subsidence, the majority of Devonian strata had reached burial depths and temperatures (above 2300 m and 160°C, respectively) necessary for gas generation. Calculated present-day maturities range from 1.4% Ro in the Exshaw Formation to 2.6% Ro in the Klua Formation for this model.

In the Cordova Embayment, the Ioe Union Shekilie A-094-Gwell well, in the southern part of the embayment, was modeled using a present-day heat-flow value of 88 mW/m^2. The burial history for this model is similar to many of the models within the Horn River Basin (Figure 15). During the Paleozoic, the Muskwa Formation reached depths of 1830 m, corresponding to a temperature of 76°C (Figure 9a). Depths remained fairly constant throughout the Permian, Triassic, and Jurassic. The Klua Formation entered the oil window in the Late Triassic and the Muskwa Formation in the early Cretaceous (at the start of foreland subsidence). Maximum burial depths and temperatures for the Muskwa Formation were of 2920 m and 183°C, respectively. During maximum burial, thermal maturity increased from 0.6 to 1.8% Ro (early-oil to wet-gas window). The thickness of the eroded section for this model is 1650 m, corresponding to an erosion rate of 55 m/m.y. Present-day maturities for the Muskwa and Klua Formations are 1.9 and 2.1% Ro, respectively (Figure 15).

In Alberta, due to shallower burial, the calculated thermal maturities are significantly lower than those calculated in the models in British Columbia (Figure 16). The 02-32-122-05W6 well, located east of 119°W was modeled with a present-day heat-flow value of 66 mW/m^2 and Devonian strata was buried to a depth of about 1400 m with a corresponding temperature of 70°C during the Paleozoic (Figure 116). As with the Cordova Embayment model, depths and temperatures stayed fairly constant from the Permian to Jurassic. Maximum foreland subsidence burial depths were 1830 m with a temperature of 92ºC for the Muskwa Formation. The Muskwa Formation did not reach the oil window until the Latest Cretaceous. The thickness of the eroded section at the 2-32 well was 525 m, corresponding to an erosion rate of 17.5 m/m.y. The present-day maturity predicated by this model is 0.62% Ro for the Muskwa Formation, with all younger strata remaining immature (Figure 16).

In all of the models, peak burial depth and temperature were reached during the Late Cretaceous and early Paleocene. However, the onset of oil generation) varies by hundreds of millions of years over the spatial extent of the study area. In the Liard Basin, the Devonian shales have been generating oil since the Carboniferous, reaching peak oil generation (transformation ratio = 50%) in the early Triassic (Figure 17). Conversely, the onset of oil generation in the Alberta wells occurred at 100 Ma at the earliest (if oil generation occurred at all), and peak generation occurred during the Late Cretaceous (Figure 17). In nearly all of the well locations modelled in this study, the transformation ratio reached 100% during foreland subsidence, which results in the current dominantly dry-gas potential nature of the Devonian petroleum system.

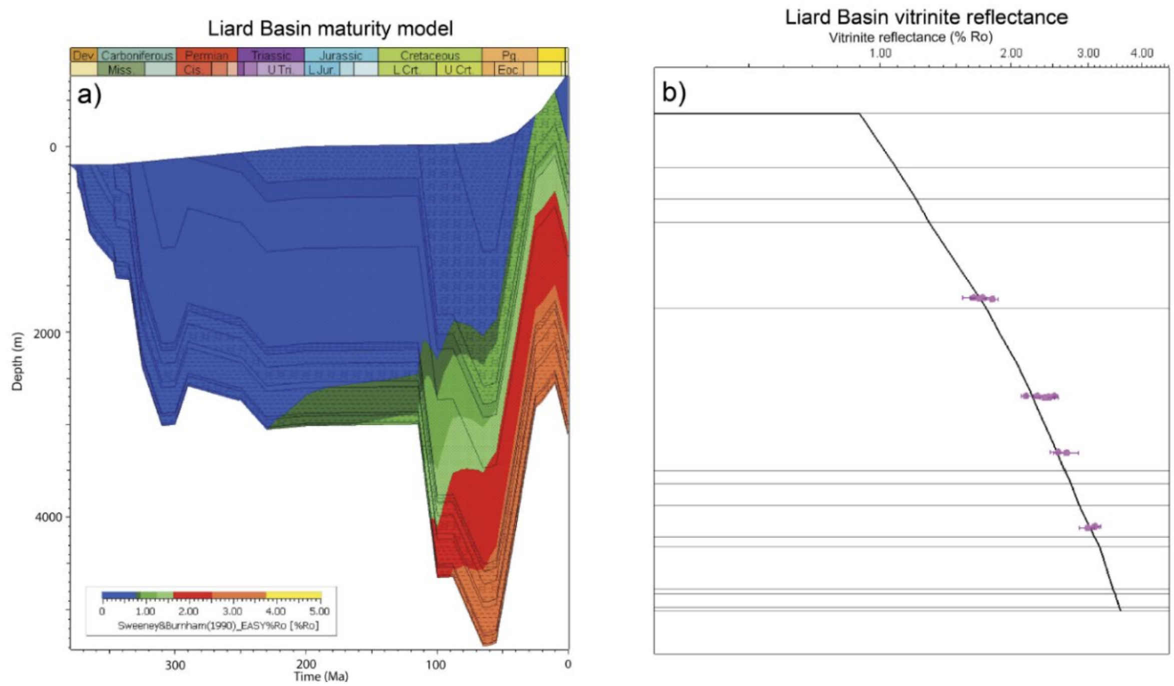

Figure 13. Liard Basin maturity model for the Nexen Beaver D-064-K well: **a)** burial-history plot with vitrinite-reflectance overlay; **b)** vitrinite-reflectance versus depth plot. The calculated vitrinite line (black) matches well with the calibration data points (pink)

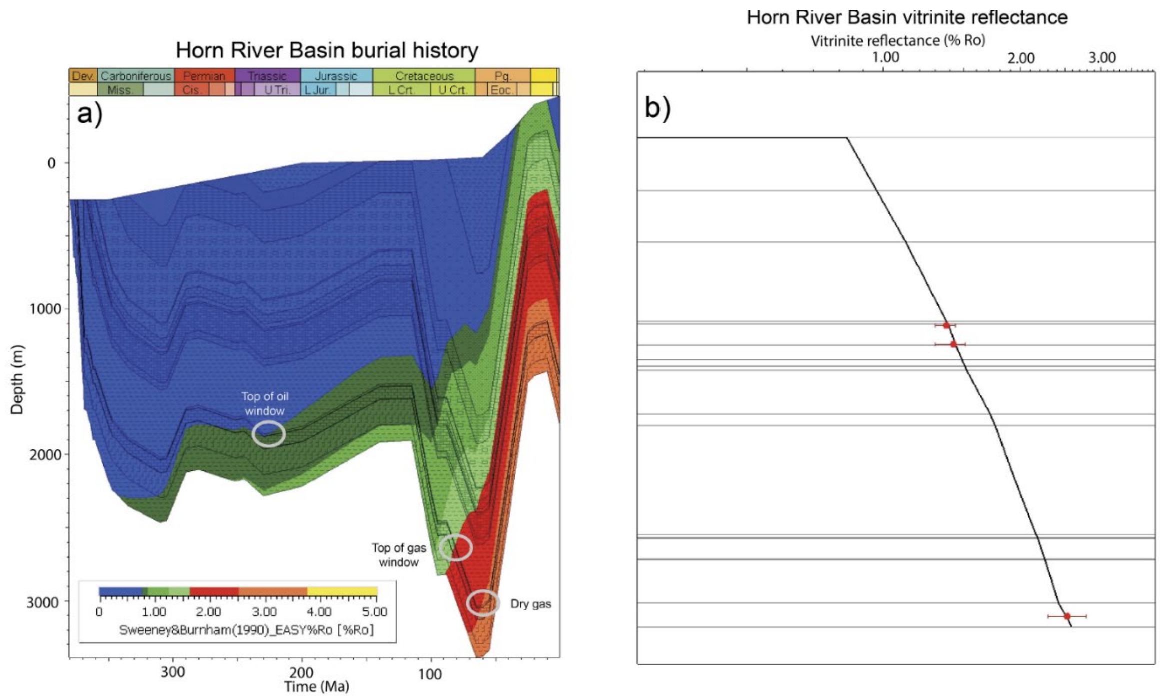

Figure 14. Horn River Basin maturity model for the Direct Gunnerl C-095-Lwell: **a)** burial-history plot with vitrinite-reflectance overlay; **b) vitrinite**-reflectance versus depth plot. The calculated vitrinite line (black) matches well with the calibration data points (red).

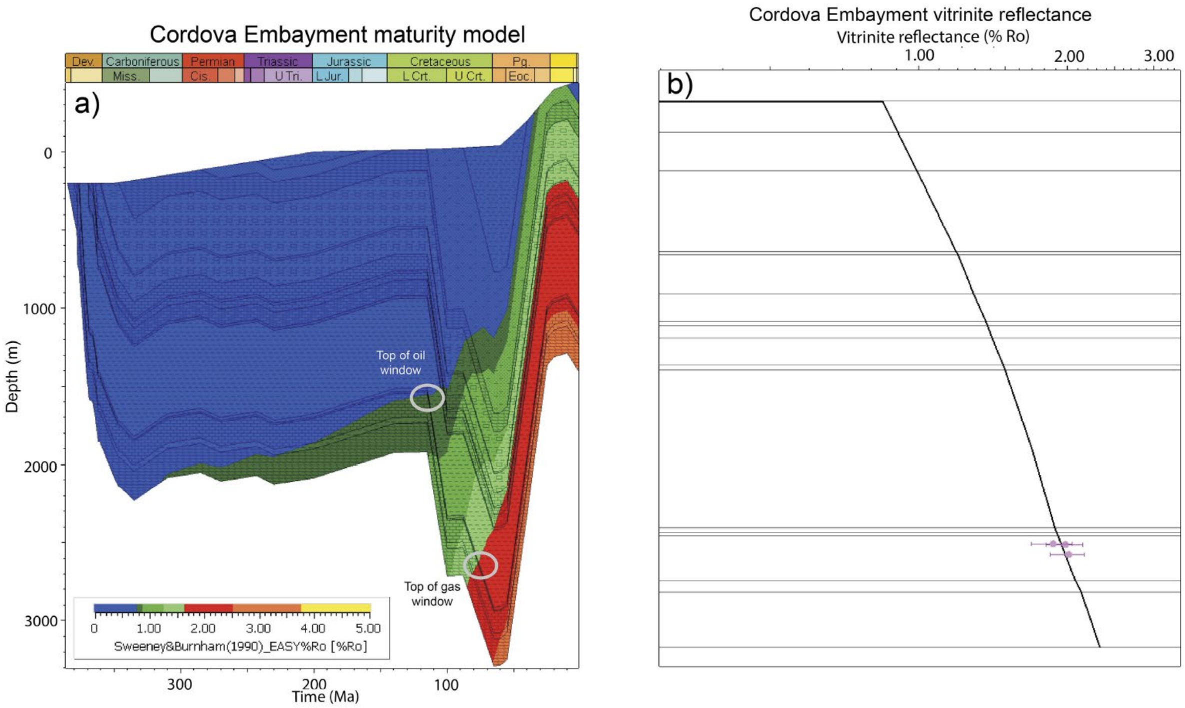

Figure 15. Cordova Embayment maturity model for the Ioe Union Shekilie A-094-G well: **a)** burial-history plot with vitrinite reflectance overlay; **b)** vitrinite-reflectance versus depth plot. The calculated vitrinite line (black) matches well with the calibration data points (pink).

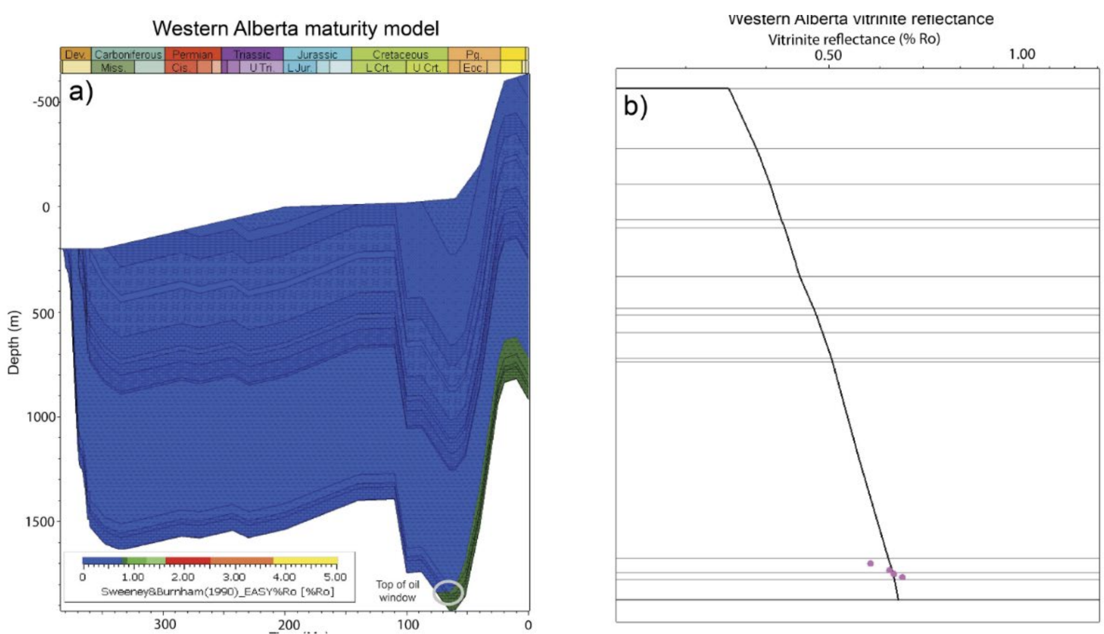

Figure 16. Western Alberta maturity model for the 100/02-32 well: **a)** burial-history plot with vitrinite-reflectance overlay; **b)** vitrinite-reflectance versus depth plot. The calculated vitrinite line (black) matches well with the calibration data points (pink).

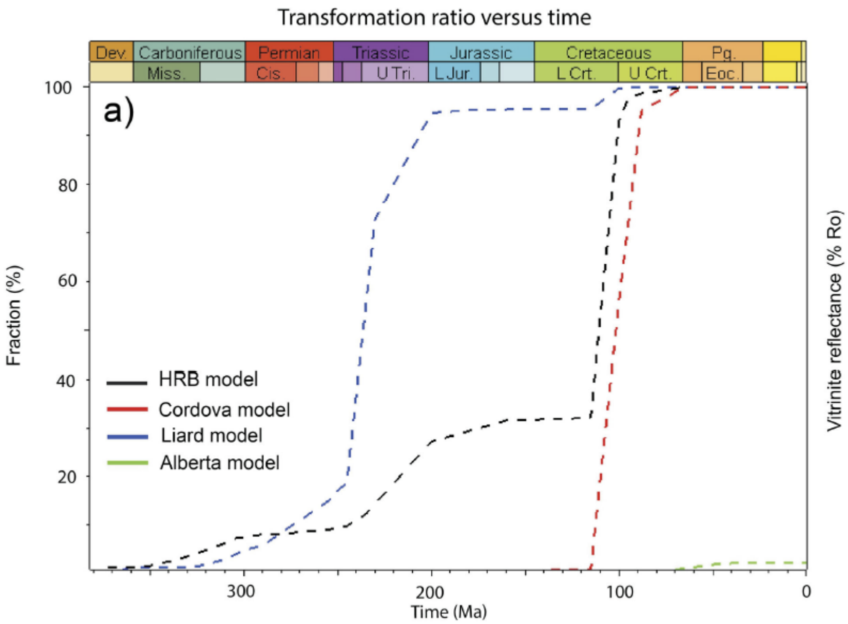

Figure 17. Relative timing of hydrocarbon transformation in the four studies areas (modified from Wilson and Bustin, 2019).

iii Reservoir Characterisation of the Duvernay Formation, a pore to basin scale study

A pore to basin scale study of the Duvernay Formation was undertaken to understand the fundamental controls on reservoir development in shales. Of particular importance was to determine how permeability of shales to liquids varies with shale diagenesis and lithofacies. The study comprised the PhD thesis research of E. Munson, which is freely available at https://open.library.ubc.ca/cIRcle/collections/ubctheses/24/items/1.0166722. Much of the following text is derived from the thesis, published research, or research in preparation for publication.

Refinement of analytical methods to characterise reservoir properties of shales- mineralogy and pore size distribution

Reservoir characteristics including porosity, permeability, and rock mechanical properties are strongly dependent on mineralogy. Hence, identifying and quantifying the mineral phases present in shales is of paramount importance. The most accepted method for quantifying mineralogy of most rocks is by X-ray diffraction (XRD) followed by Rietveld analysis. For quantitative XRD analysis, it has been shown that minerals must be crushed to an ultra-fine particle size with a micronizer, homogenized, and the sample prepared without preferred orientation of the crystals. Preparing samples in this fashion is tedious and expensive, although shown to be necessary for quantitative analysis. It is generally accepted that if analysis results fall within ± 3 wt. % absolute of a known composition at the 95% confidence level they are considered to be 'highly accurate' (Hillier, 2000). Since we recognize that in most true shales, by definition, the particle size is already ultra-fine, we experimented with various sample preparation techniques. In this study (Munson et al., 2016), we show that the total absolute error between the commonly accepted spray dry method of sample preparation and our method of hand grinding the shale samples and preparing simple smear mounts for fine-grained reservoir rocks is ± 2.6 wt. % at the 99.6 % confidence level (3 standard deviations), thus within the ± 3 wt. % guideline. We further validated our methods by quantifying samples of known mineralogy for comparison with the more expensive and time consuming micronizing and spray dry and back mount techniques (Figure 18).

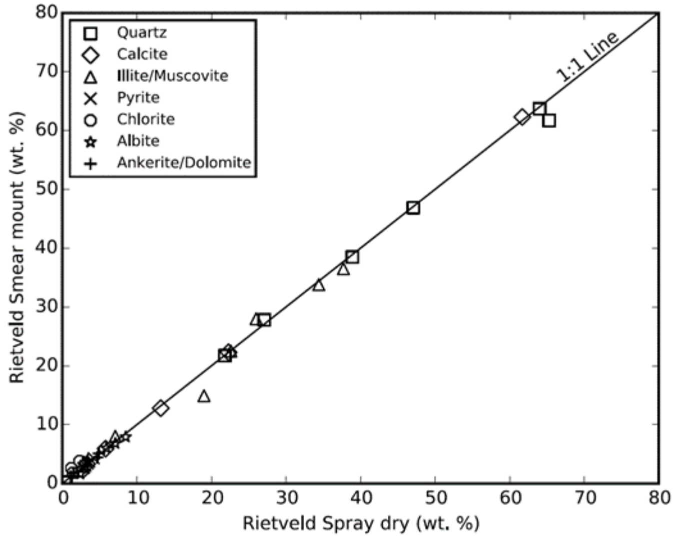

Figure 18. Spray dry weight percent versus smear mount weight percent by individual phases. The line is a 1:1 ratio.

Critical to our studies was characterising the capillary pressures of the shales through analyses of pore (throat) size distribution, wettability, and surface and interfacial tension of fluids. To this end we utilised mercury intrusion porosimetry (MIP) which is a standard procedure for study of porous media. For rocks with ultra fine pore throats such as shales however, this technique produces significant errors due to conformity at low pressures if crushed particles are used and sample compression at the high pressures required to access small pore throats (Figure 19). To provide more reliable data for shales we developed novel techniques to analyze MIP data to generate consistent, error-limited results as well as additional rock property data apart from the usual MIP derived parameters. In our study we confirmed the closure correction for tight rocks proposed by Bailey (2009) and investigated by Comisky et al. (2011) and expand on Bailey (2011) to: (1) correct incremental intrusion curves for pore volume lost due to compression and (2) account for incremental intrusion that occurs concurrent with compression. In addition, we develop a new calculation for stressed porosity using MIP compression data to correct unconfined porosity measurements for any net confining stress desired. We further documented the effect of sample size on closure and show the effects of closure and compression on commonly reported MIP parameters such as “Swanson” permeability.

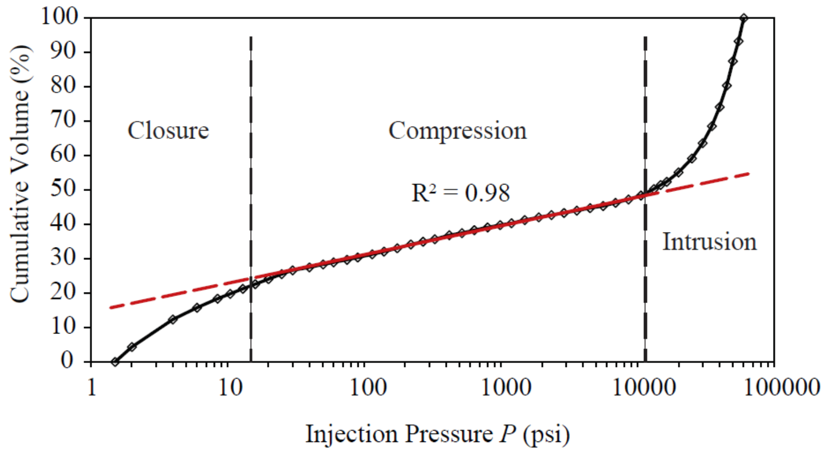

Figure 19. Semi-log cumulative intrusion plot for a typical mudstone sample. Red line is a power law fit over the interval attributed to compression. Where the fit deviates it is due to closure (at low pressure) or intrusion (at high injection pressure).

Impact of thermal maturity and compaction on the pore size distribution and matrix permeability in the shale gas and shale oil producing Duvernay Formation

The goal of this study was to investigate the influence of compaction and thermal maturity on the pore structure evolution of organic-rich, shale gas and shale oil producing reservoir rocks. The Duvernay Formation is well suited for this study because the formation spans multiple thermal maturity boundaries from immature to overmature with increasing burial depth, and is generally compositionally similar over this range of maturity. Sampling was performed over the entire range of thermal maturities, which enables the comparison of pore structure versus maturity from samples with the same depositional environment, mineral provenance, and organic matter type. In the study, MIP, nitrogen, and carbon dioxide low-pressure gas supplemented with field emission scanning electron microscopy imaging were used to investigate the pore structure, which was then correlated with matrix permeability to gas and oil.

Comparison of pore structures from samples of varying maturity provided insight into the impact of thermal maturity and compaction on mudrock microstructure and permeability (Figure 20). Organic-matter hosted, fine mesoporosity is visible with FE-SEM imaging from the onset of the oil window (HI = 348 mg HC/g TOC) and the development of organic matter-hosted pores increases in both size and abundance systematically with increasing maturity into the dry gas window. The pore size distribution, as measured by N_2 low pressure gas adsorption, shows a progressive increase in fine pore sizes with thermal maturity from the oil window through the dry gas window and the subsequent loss of larger pore modes. Macropore volumes are highest within the shallow, immature samples and progressively decrease with increasing maturity and burial due to compaction. Average helium pulse-decay permeability for samples from the wet gas and dry gas window are an order of magnitude higher than oil window samples. In general, this is a result of the development of fine pore sizes with maturity associated with organic matter.

Within the wet gas window, permeability is dominantly controlled by the coarse meso- to macropore size fraction, which is associated with increased total quartz and feldspar content. The permeability for dry gas window samples is controlled by higher fine pore volumes correlated to relatively higher total clay and quartz and feldspar content.

Gas expansion porosity and permeability, which probes the total gas uptake by the matrix is well suited to measuring the permeability of finer pore sizes and characterises the fine pore sizes which are sufficiently interconnected to be permeable. Oil window samples have lower gas expansion porosity and permeability, whereas wet gas and dry gas window samples have higher permeability and a higher proportion of fine pore volumes.

The contact angle of water in air increases with increasing organic matter content since the organic mater (and organic matter-hosted pores) are hydrophobic and mineral surfaces are hydrophilic.

The pulse decay permeability to oil is lower than that of helium, which is interpreted to be due to wettability variations within the pore structure. The oil permeability values show no direct correlation to composition due to the complex nature of the pore system, which is composed of pores of varying sizes, spatial distributions, and pore wall compositions that have varying wettability.

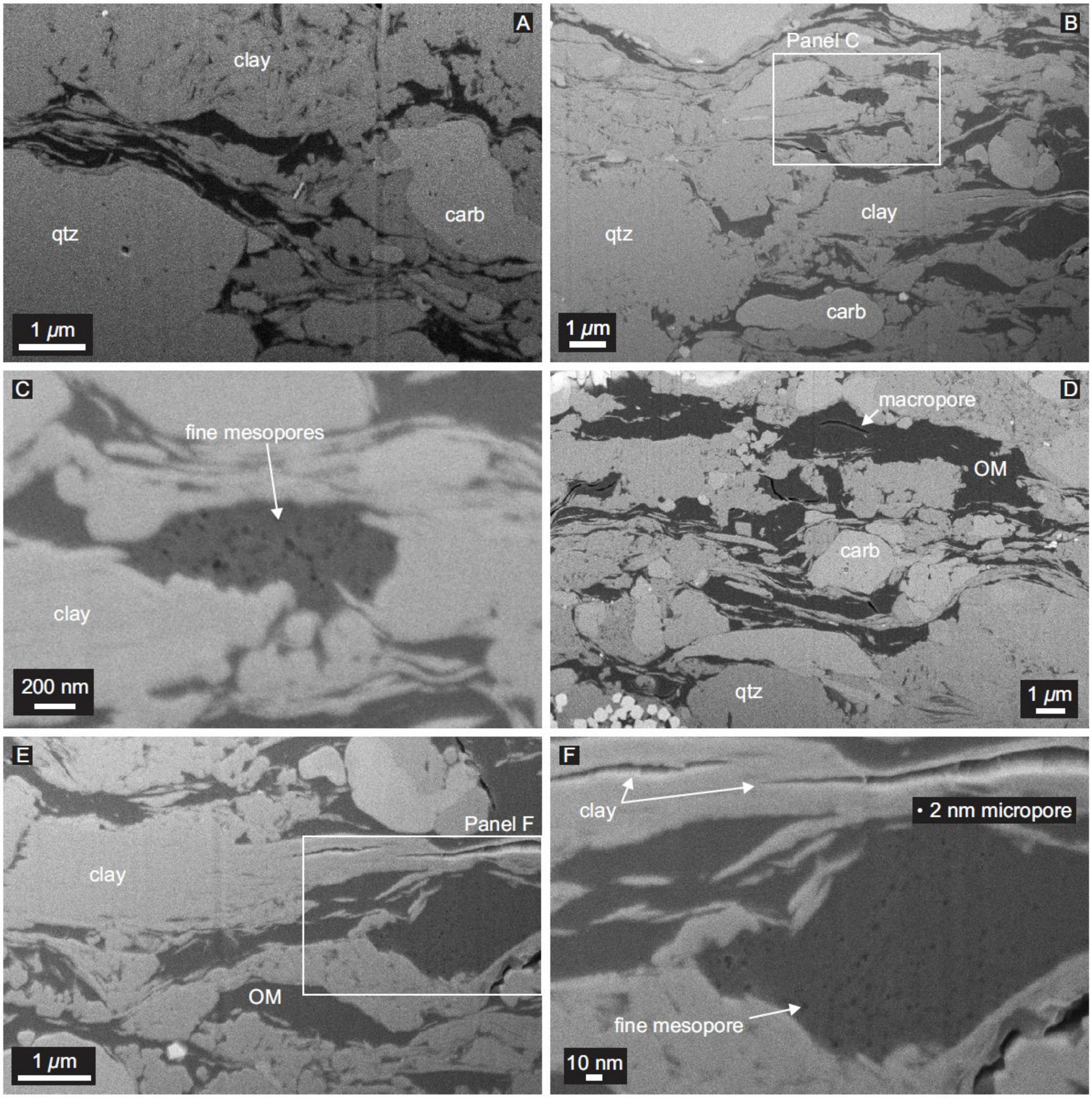

Figure 20, Texture and porosity associations from FE-SEM for early oil window Duvernay shale. Organic matter is generally non-porous, however fine mesopores (C) and coarse micropores (D) were imaged in two separate locations. Macropores exist in crack-like distributions within or at the boundaries of OM particles (D). Intra-particle clay hosted porosity is also evident (E).

Regional reservoir characterization model for the shale gas and shale oil producing Duvernay Formation: Regional reservoir distribution and reservoir properties using wireline log signatures and high-resolution laboratory data

In this study, the regional distribution of reservoir facies of the Duvernay Formation was investigated. Reservoir characteristics including mineralogy, total porosity, organic matter (OM) content, net reservoir thickness, potential fracture barriers or baffles, reservoir quality impairments, and the impact of reef development on reservoir quality were investigated and mapped through use of wireline logs calibrated with laboratory measurements and artificial neural network modeling.

The Duvernay Formation currently dips to the southwest with subsea depths ranging in the study area from about 450 m in the northeast to 3100 in the southwest Pembina area. In general, regional organic maturity trends coincide with current burial depth. The Duvernay is immature in the northeastern portion of the basin (0.4 – 0.6 %Ro, Stasiuk and Fowler, 2002; Tmax 415 – 420 °C, this study) and increases in maturity to the southwest where it is overmature (1.8 – 2.4 %Ro, Stasiuk and Fowler, 2002, Figure 21). Locally, maturity trends are more complex and may be related to variable basement heat flow (Davis and Karlen, 2013). More research is needed to precisely delineate boundaries of dry gas, wet gas, condensate, and volatile oil hydrocarbon zones. Average Rock Eval derived hydrogen index values (HI) for the Duvernay are consistent with values anticipated based on Tmax data and vitrinite reflectance values (Figure 22). Local deviations in HI that do not conform to maturity values may be due to variations in organic matter type. Total Duvernay porosity shows a positive correlation to total quartz content, a moderate negative correlation to total carbonate content at higher carbonate concentrations (> 40%), a poor negative correlation with TOC content, and no systematic trend with maturity.

Well-bore measured pore pressures indicate the Duvernay Formation is over pressured (12.0 kPa/m to 20.2 kPa/m). In general, pore pressure and reservoir temperatures correlate with present day burial depth; however, notable exceptions exist, which do not follow depth based models (see Munson, 2015, https://open.library.ubc.ca/cIRcle/collections/ubctheses/24/items/1.0166722). Local variations in Duvernay pore pressure and temperature are important in that they correspond to areas of increased hydrocarbon storage and production potential. Some temperature variations correlate to basement scale heat flow and generally align with structural lineaments determined from gravity anomaly data.

Isopach maps of the major stratigraphic units are provided in Munson (2015, https://open.library.ubc.ca/cIRcle/collections/ubctheses/24/items/1.0166722). Deposition of the Majeau Lake and lower Duvernay may have occurred concurrent during the initial sea level transgression, independent of Leduc reef development. Lower Duvernay thicknesses increase in the more distal portions of the basin, while Majeau Lake thicknesses increase toward the basin center. The lower Duvernay may thus represent the toe of Majeau Lake clinoforms.

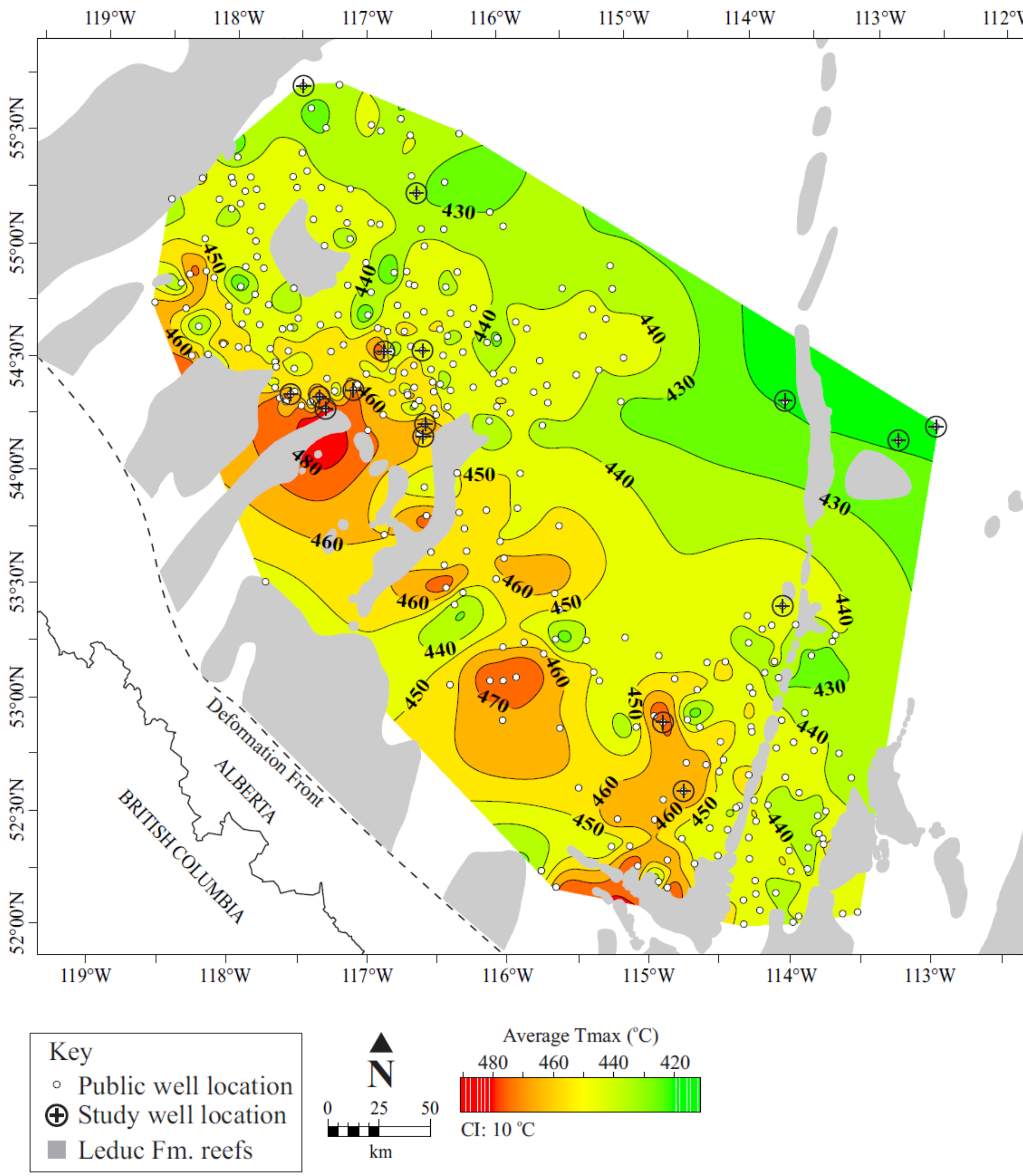

Figure 21 Average Duvernay Formation Tmax from publicly available data and data generated for this study.

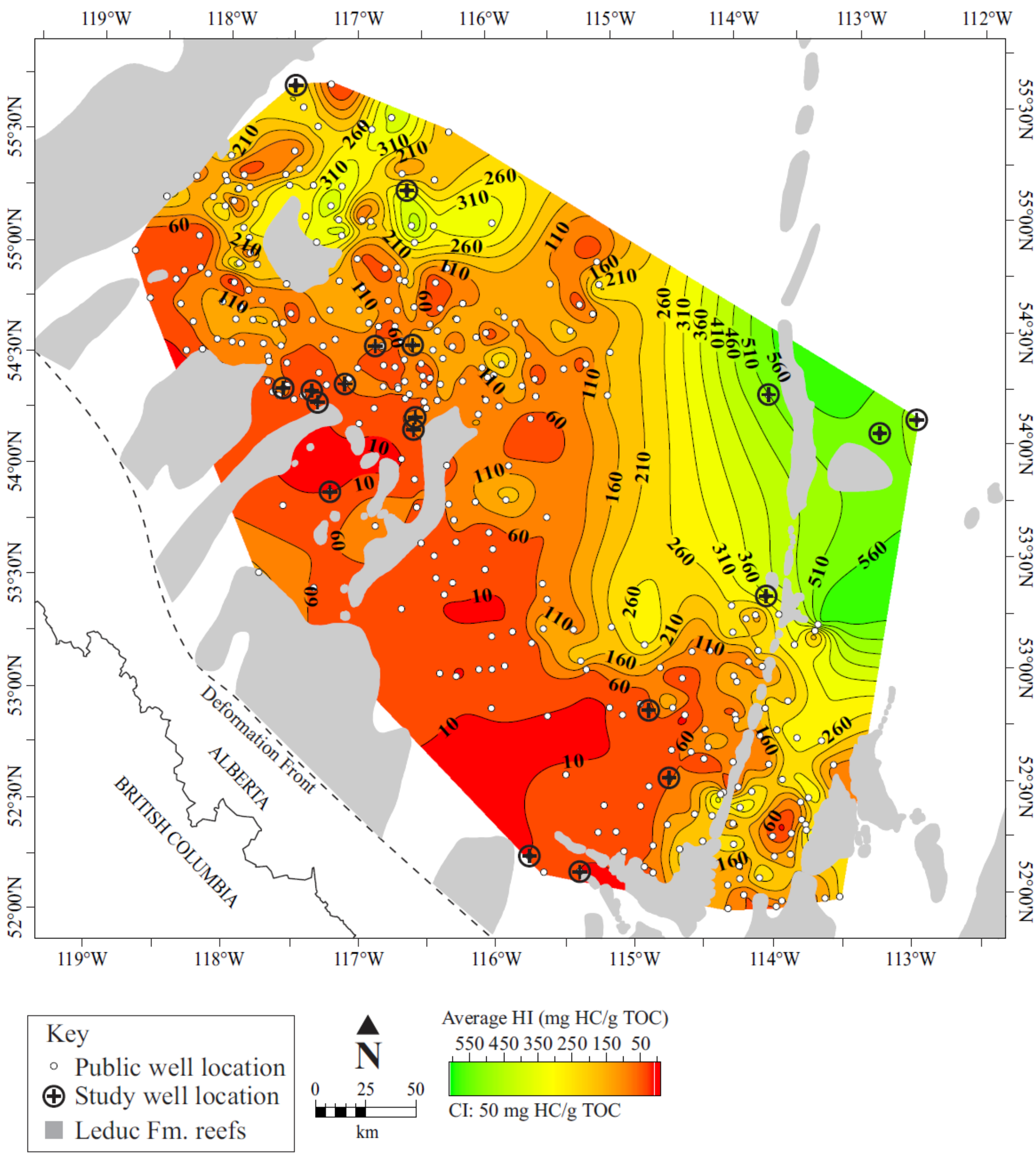

Figure 22. Average Duvernay HI from publicly available data and data generated for this study.

The middle carbonate unit of the Duvernay has poor reservoir production and storage potential due to low porosity and low TOC contents. The thickness of the middle carbonate unit increases basinwards from Leduc reef accumulations and may represent a prograding carbonate ramp developed during a high stand. The middle carbonate dominates the Duvernay section in the basin center, reaching thicknesses over 40 metres. Increased thickness of the middle carbonate negatively impacts total reservoir thickness and may be a hydraulic fracture barrier.

Reef development is the dominant control on the distribution of upper Duvernay organic-rich mudstones. Increased mudstone thicknesses occur in inter-reef embayments where basinal water circulation would have been the most restricted. On the basinward side of reefs, Duvernay lithofacies are thinner, highlighting the circulation-restriction effect of reef complexes. Reef-derived debris flow units locally increase total Duvernay thickness, but are detrimental to overall reservoir quality. Reef-debris lithofacies have low hydrocarbon production and storage potential due to low TOC and low total porosity. Reef debris flows can occur in multiple discrete units, which subdivide organic-rich mudstone lithofacies. Therefore, reef debris units, where thick, pose hydraulic fracture propagation issues, if significant mudstone thicknesses are available for production. Mudstones interbedded with debris flow units have greater TOC, but significantly less porosity and in general are of poorer reservoir quality than typical reservoir mudstones, unassociated with debris flow units.

In order to extrapolate laboratory measurements on core to areas with no core control, artificial neural network (ANN) models were used to calibrate laboratory analyses to wireline log suites. Models were developed for total organic carbon content, quartz, carbonate, and porosity in the Duvernay and other units. Based on the ANN, the TOC content of Duvernay rocks is significantly higher within localized embayments of Leduc reef complexes compared with more basinward deposits (Figure 23). While restricted basinal circulation, due to Leduc reef development, is favored as the mechanism for preservation of organic matter within Duvernay sediments as a whole, the effect is particularly pronounced within the sheltered embayments. This may lead to increased hydrocarbon saturations and greater volumes of OM-hosted porosity in these areas, which are positive reservoir characteristics.

The average quartz content increases toward the basin center, which is attributed to a reduced input of reef-derived carbonate components. No other dominant regional trends in quartz content occur. The lack of depositional trends is likely due to the varying mode of occurrence of quartz within Duvernay rocks and particularly the inability to distinguish biogenic versus detrital quartz based on logs.

Total average carbonate content increases slightly towards the basin center (up to 25 % average carbonate content per well). This indicates that a significant component of the carbonate within the Duvernay is inter-basinal and is being transported from carbonate sources other than the local reef developments. A possible source could be the carbonate platforms developed to the east during Duvernay deposition (Switzer et al., 1994). However, average carbonate content within Duvernay mudstones (excluding reef debris flows) does not vary significantly within the study area (from 10 – 25 % average carbonate content), which may be obscuring regional trends. The presence of local, discontinuous limestone interbeds could also impact the calculated average carbonate content within a given well. Multiple wells containing reef-derived debris flows are identified by increased average carbonate content (typically greater than 50 % average for the section; Figure 6.12). From a regional perspective, the ability to quickly identify potential areas of debris flow units will assist in risk assessment to reservoir hazards.

Porosity is controlled by mineralogy and organic matter content, which creates a unique mudrock reservoir texture that varies with thermal maturity and burial. Therefore, regional trends in porosity are based on the interplay of these components (Figure 24). However, no dominant regional porosity trends are clear. Average porosity generally decreases proximal to Leduc reefs perhaps due to the input of reef-derived carbonate and the negative correlation of calcite and total porosity. Regions of greater porosity generally coincide with greater average quartz content but there are many exceptions. In general, the distribution of average porosity is controlled by local sedimentological factors along with the complex interplay of thermal maturation and burial, which is not directly evident in regional maps.

The relationships of mineralogy, TOC, porosity, and mudstone reservoir thickness to reservoir quality creates a spectrum of variably favorable reservoir rocks based on the interplay of these variables and their individual relationships to reservoir quality. Since reservoir quality within the Duvernay varies with few natural and explicit lithologic cutoff points (e.g. beds of consistent lithology, such as limestone beds), discrete reservoir quality gradations are defined for this study to highlight areas of most-prospective reservoir along with areas of lesser potential. The reservoir quality gradations are based on metrics considered to be important for Duvernay mudstones. Three reservoir quality gradations were defined using cutoff values of the mineralogy, TOC, and porosity ANN models created for the Duvernay. Model 1 represents the best quality reservoir rocks as determined in this study. Reservoir rocks which fulfill the criteria for model 1 must have > 50 % quartz, < 30 % carbonate, > 3 % TOC content, and > 4 % porosity (Figure 25). These parameters were chosen based on the positive relationship of total quartz content to porosity, brittleness, and permeability; the positive correlation of porosity to hydrocarbon storage; the positive correlation of TOC to hydrocarbon generation potential; and the negative relationship of carbonate content to porosity, TOC, and potential fracture barriers (as discrete beds). The total thickness of Duvernay mudrocks, which fulfill the criteria for each model, was then mapped to determine the regional distribution of prospective reservoir facies.

Regional maps of reservoir quality models 1, 2, and 3 are given in figures 25, 26, and 27. Since model 1 was designed to represent the highest quality reservoir, it is the most restrictive and shows the smallest thickness and distribution of facies meeting the criteria. Model 2 represents all reservoir facies of good quality (and best quality) and the thickness and distribution are significantly greater than model 1. Model 3 was designed with the least restrictive criteria and most mudstone facies, exclusive of discrete limestone beds, meet the criteria. The distribution of facies for model 3 is similar to model 2; however, the thickness of strata which meet the criteria for model 3 is significantly greater as model 3 is the least restrictive,

As the Duvernay Formation is progressively developed as an unconventional resource and new data is available, undoubtedly the criteria for grading reservoir quality will change based on well performance.

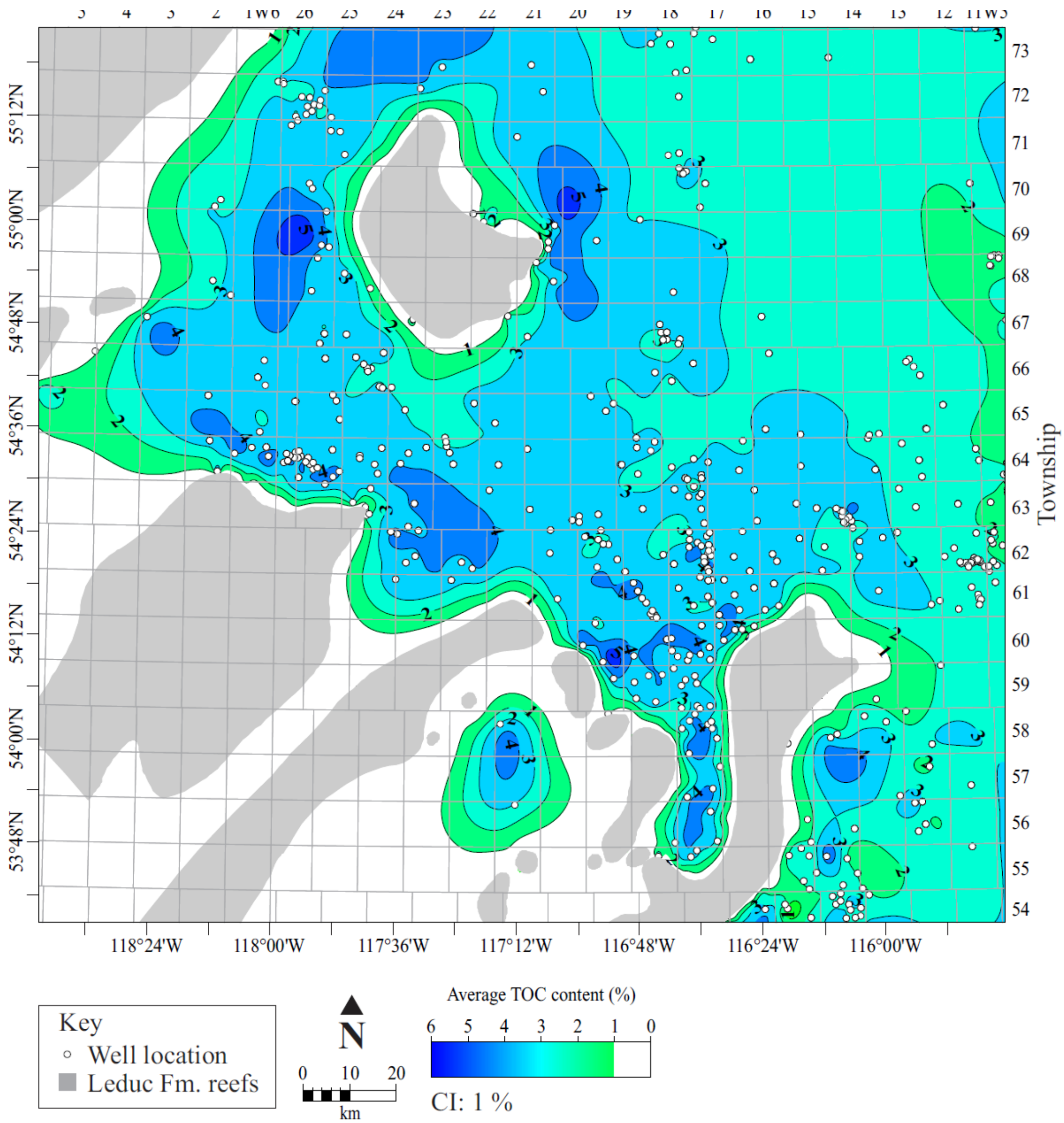

Figure 23 Average TOC content for the upper and lower Duvernay.

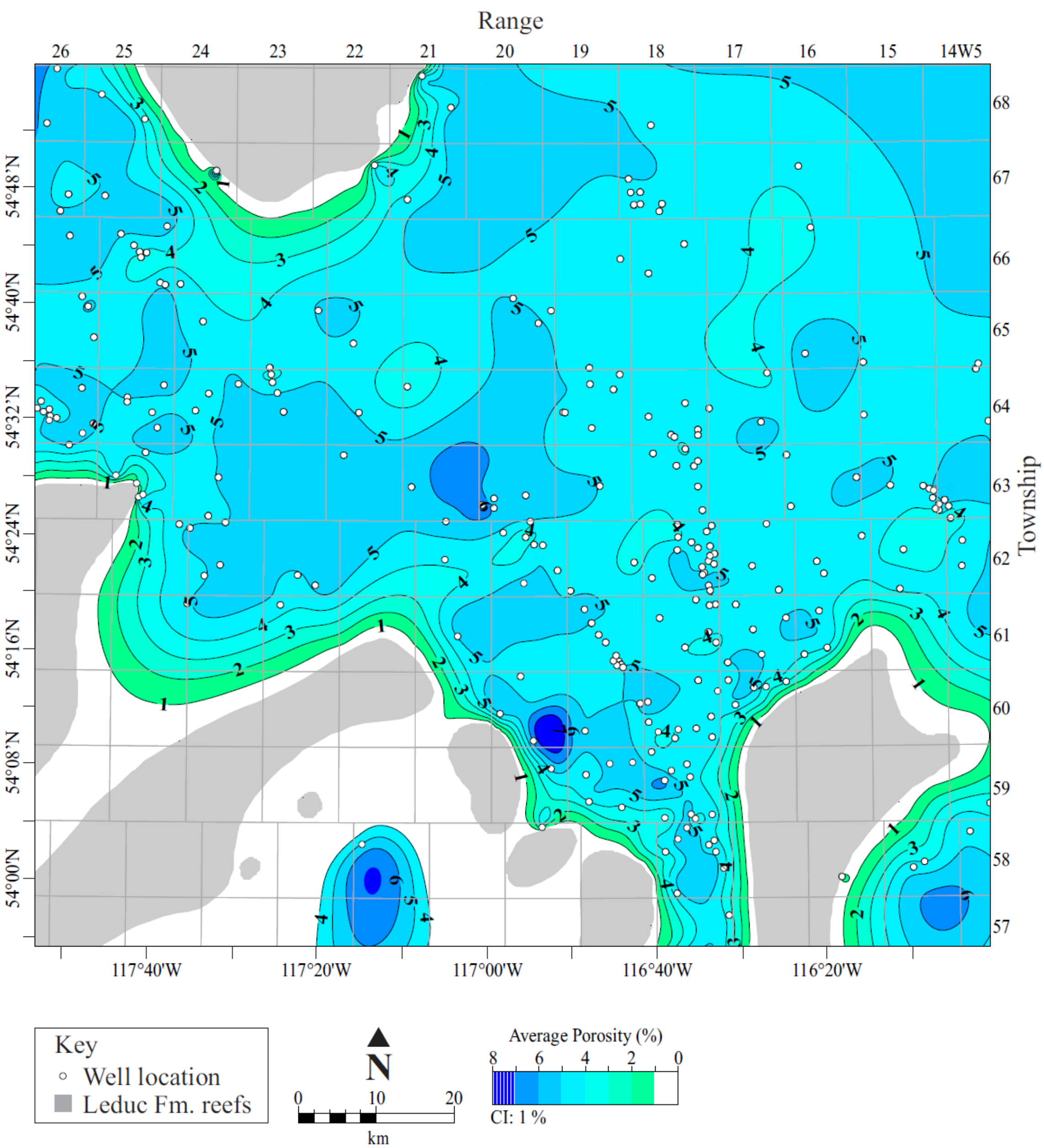

Figure 24. Average porosity for the upper and lower Duvernay. Reefs are zeroed contoured; white is < 1 % porosity or areas of no data.

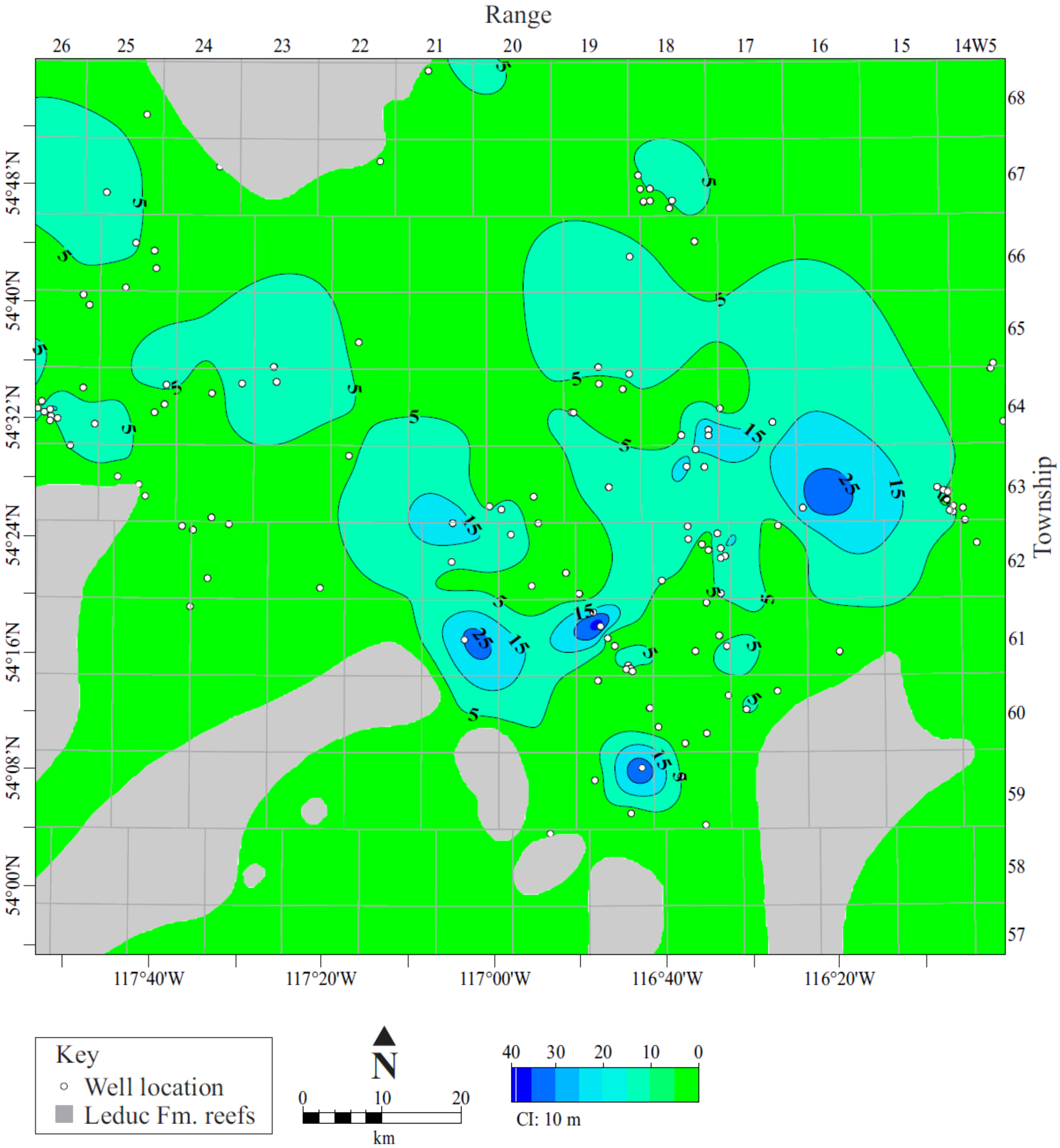

Figure 25. Total thickness of Duvernay mudrocks which satisfy the criteria for reservoir quality model #1

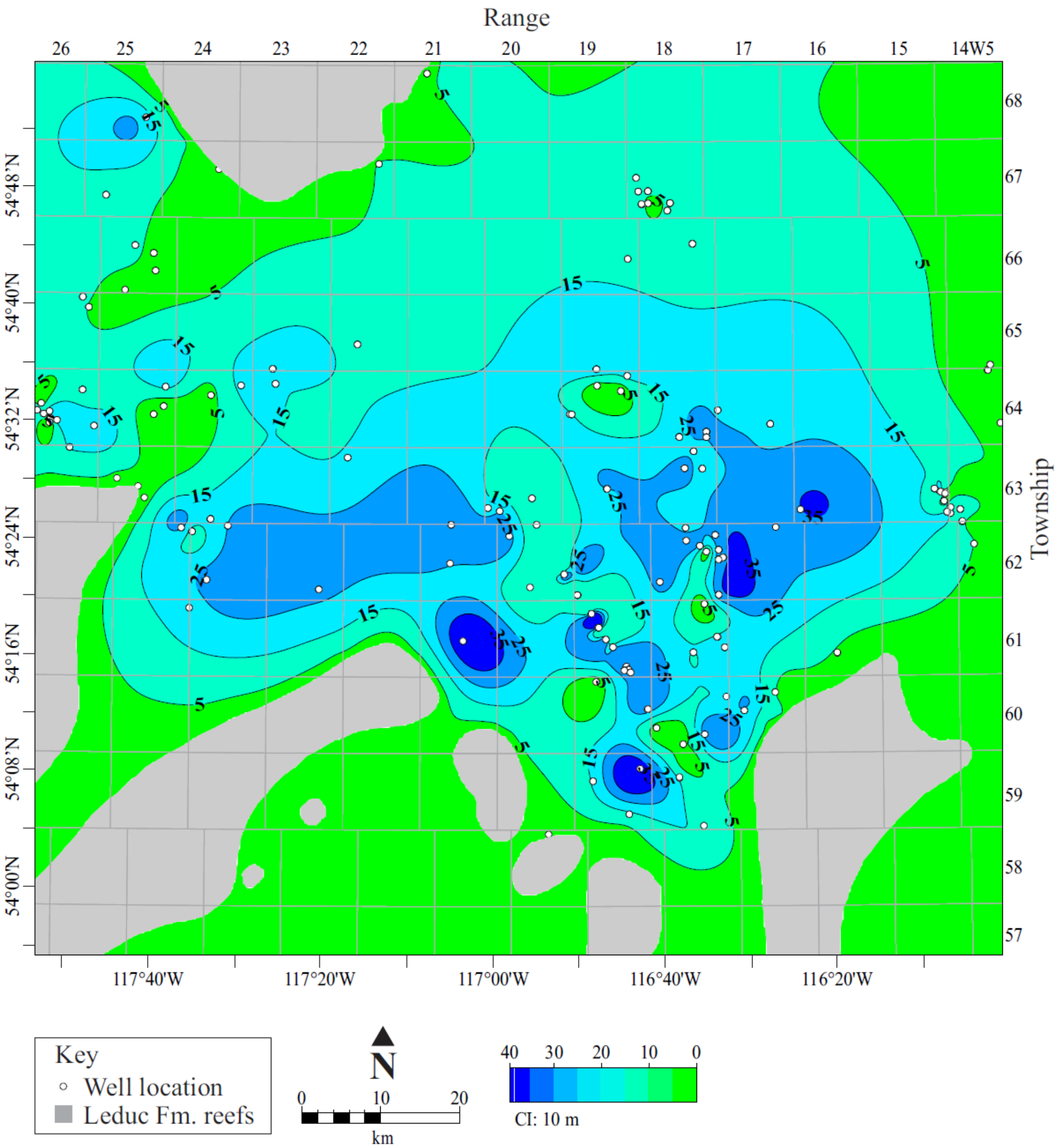

Figure 26. Total thickness of Duvernay mudrocks which satisfy the criteria for reservoir model # 2 (Table 6.2).

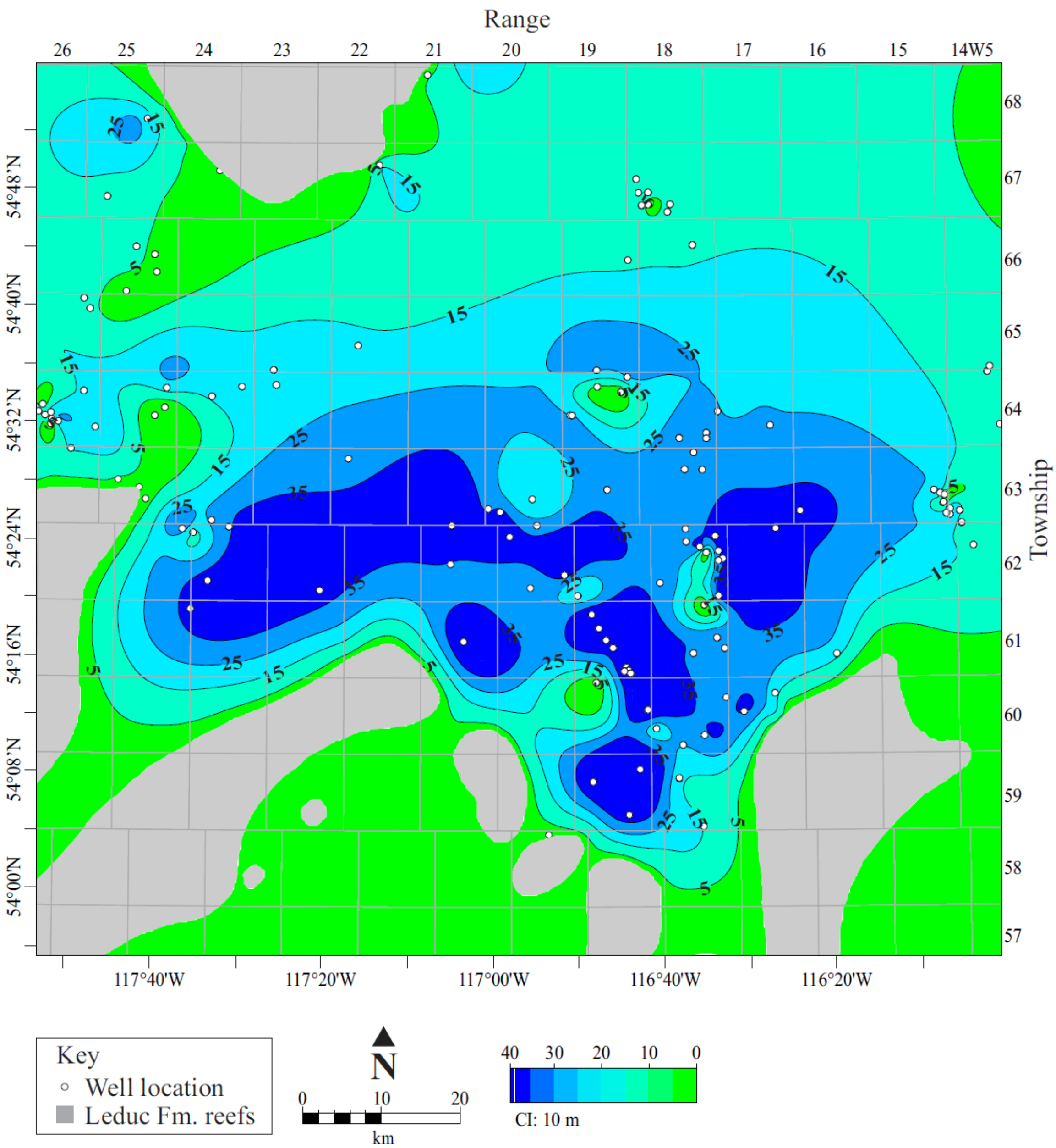

Figure 27. Total thickness of Duvernay mudrocks which satisfy the criteria for reservoir model #3 (Table 6.2).

iv Petroleum System Analyses of the Doig Formation, Northeastern British Columbia

Characterizing the Doig Formation through a petroleum system analysis approach was a major goal of this research proposal. The Doig Formation, although locally developed as a conventional reservoir, is considered a prospective unconventional target, which has largely been overlooked due to the greater prospectivity of the underlying Montney Formation. Our research on the Doig Formation comprises the PhD thesis research of P. Lacerda Silva which is in progress. This study has mapped the spatial distribution of lithofacies, total organic carbon content, organic matter quality, mineralogy, porosity and permeability on a regional scale in northeastern British Columbia. Detailed wire line interpretations calibrated to core analyses have facilitated extrapolating facies, geochemistry, and geomechanical properties to non-cored areas. Petroleum system modeling will be used to reconstruct and determine the timing of thermogenic hydrocarbon generation, migration, expulsion, and retention.

The study has focused on 24 cored wells distributed across the entire extent of the Doig Formation. Analyses from these wells have been used to calibrate wireline logs. The Doig organic matter shows a wide range of hydrogen index (HI) and thermal maturity values, spanning from immature to overmature (Figure 28). Thermal maturity was mapped from suitable pyrolysis Tmax values (Figure 28). A wide range of HI values for similar Tmax values through the oil window suggests that multiple types of kerogen are present in the Doig, from type II, through type II-III to type III (Figure 29). This conclusion differs from other studies that found mostly type II kerogen in the Doig (Riediger et al., 1990; Ibrahimbas and Riediger, 2004; Walsh et al., 2006). Combining maturity and shale thickness maps suggests that one third of the Doig gross rock volume lies within the condensate/wet gas window for type II kerogen. The vast majority of this area is in British Columbia.

A log-based TOC transform was performed on 200 wells for which laboratory data and a minimum well log suite (compressional slowness and resistivity) were available. The methods used are described by Passey et al., (1990), and Carpentier et al., (1991), and the parameters were adjusted iteratively in order to match the laboratory calibration data. Both methods had acceptable results, as assessed by the subtraction of log-derived TOC value from the laboratory-derived TOC. However, depth shifts, log resolution, depth shifts, and the influence of migrated hydrocarbons on resistivity contribute to errors in values calculated by these methods (Figure 30). Ongoing work will improve on the quality of the TOC transform, increasing the confidence in the models; this will allow extending the TOC calculation to wells without laboratory data, resulting in a denser grid of data and a TOC map with enhanced resolution and accuracy. Historic production data will be integrated into the analysis and cross-correlated with the maturity maps to investigate the influence of kerogen type on the type of hydrocarbons generated.

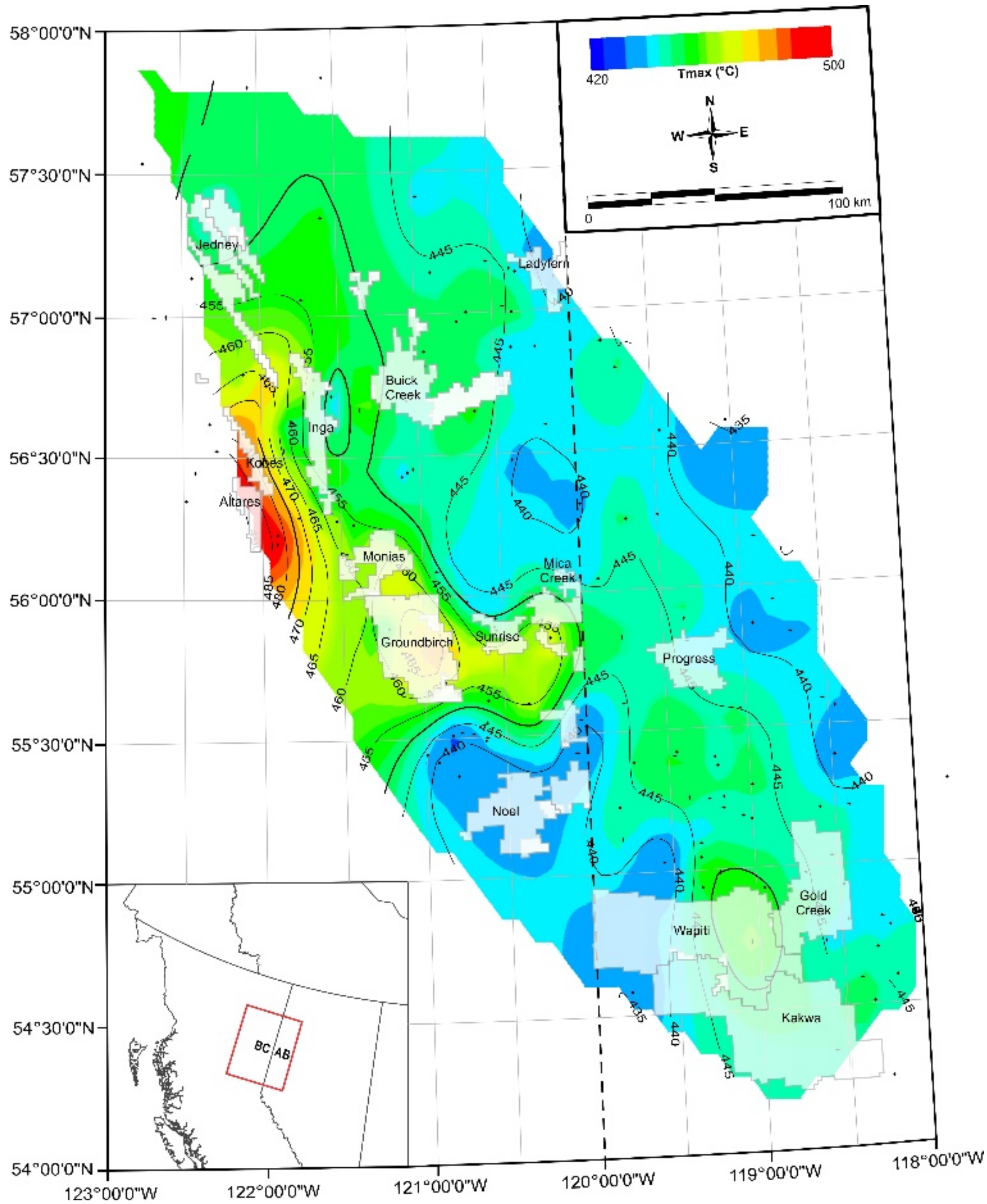

Figure 28. Generalized thermal maturity map of the Doig interval, expressed by Tmax.

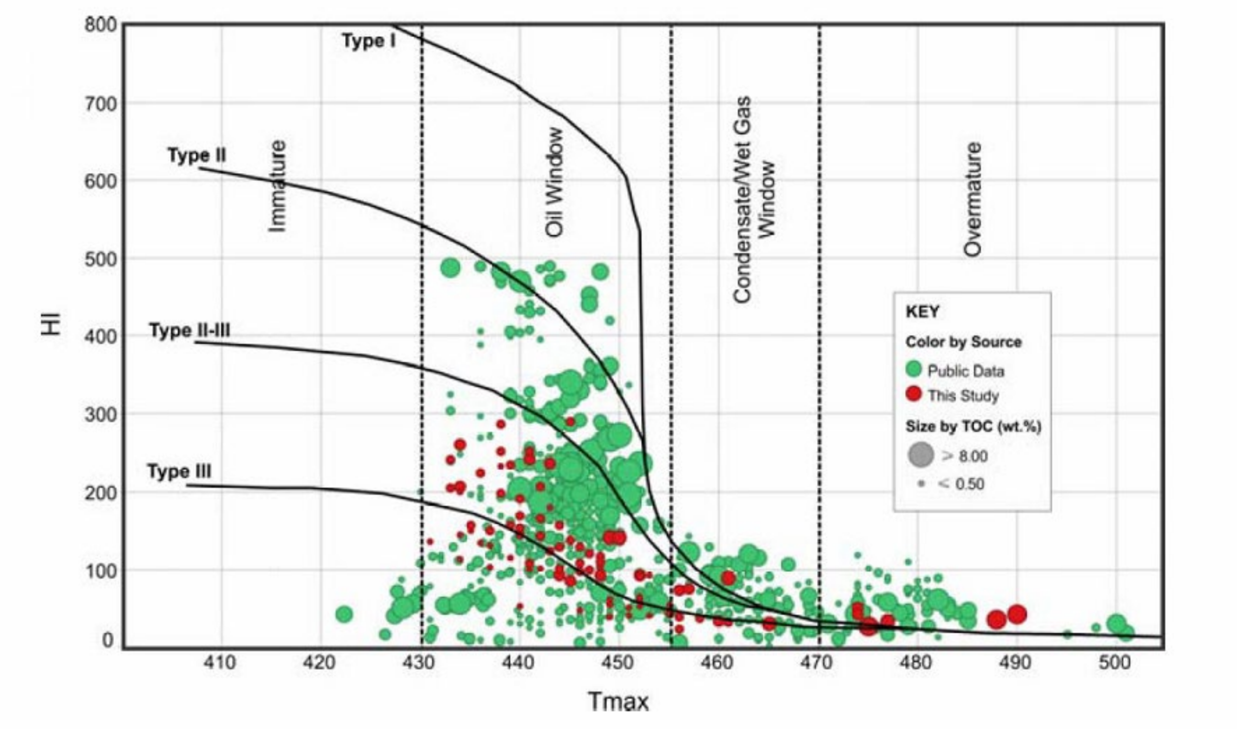

Figure 29. Tmax and HI crossplot of pyrolysis data from public domain and generated for this study, colour coded by data source, sized by TOC. Only data points that either presented a good quality S2 peak or consistent Tmax values are shown.

The mineralogy, porosity, pore size distribution, and permeability of the Doig vary with lithofacies and aerially an stratigraphically There is a large spread in matrix permeability, spanning four orders of magnitude from 10^{-5} to 10^{-1} millidarcies (mD), for a porosity range of less than 1% to nearly 15% (Figure 31), and enough variability within each lithofacies to cause a matrix permeability range spanning multiple orders of magnitude in vertical distances shorter than 20 cm. The permeability of the Doig is controlled by a complex interplay between total porosity, pore-size distribution, and clay content. Despite the large spread in porosity for a given permeability interval, porosity is still the best single predictor for permeability. Pore-size distribution and, more subordinately, clay content comprise a second order control on permeability.

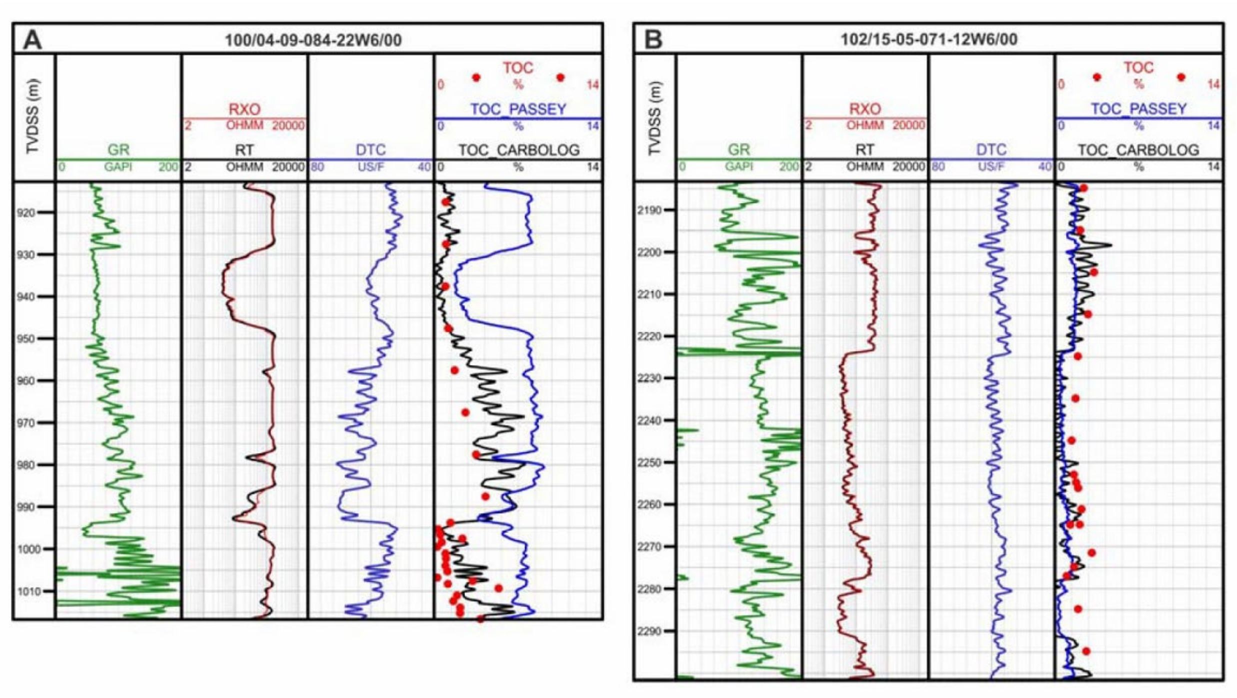

Figure 30. Log plots of two wells (A and B). from left to right on each well: vertical depth below sea level, gamma ray (track 1), resistivity (track 2), compressional sonic slowness (track 3), TOC (track 4), showing good agreement with laboratory data (red circles on right-most track) of one method in both wells, while the other method largely overestimates TOC on well A.

Based on flow capacity, the Doig lithofacies can be divided into two groups: rocks with porosity larger than 5% having permeabilities of 10^{-3} to 10^{-1} mD that are essentially composed of quartz-rich siltstone to very fine sandstone (illustrated by samples TG19 and TB1; Figure 31) and phosphatic, oolitic packstone to grainstone (illustrated by samples CD15 and MH7). The rocks of the second group have porosities ranging from just under 1% to 5% and a larger spread in permeability, ranging from 10^{-5} to 10^{-1} mD. This spread is attributed to enhanced permeability due to microfractures and degrades the correlation between porosity and permeability. The phosphatic, oolitic packstone and grainstone of the basal Doig and the quartz-rich siltstone of the upper Doig have the highest porosity and more favorable balance of macro- to meso-pores, which make these lithofacies the best reservoirs in terms of flow capacity.

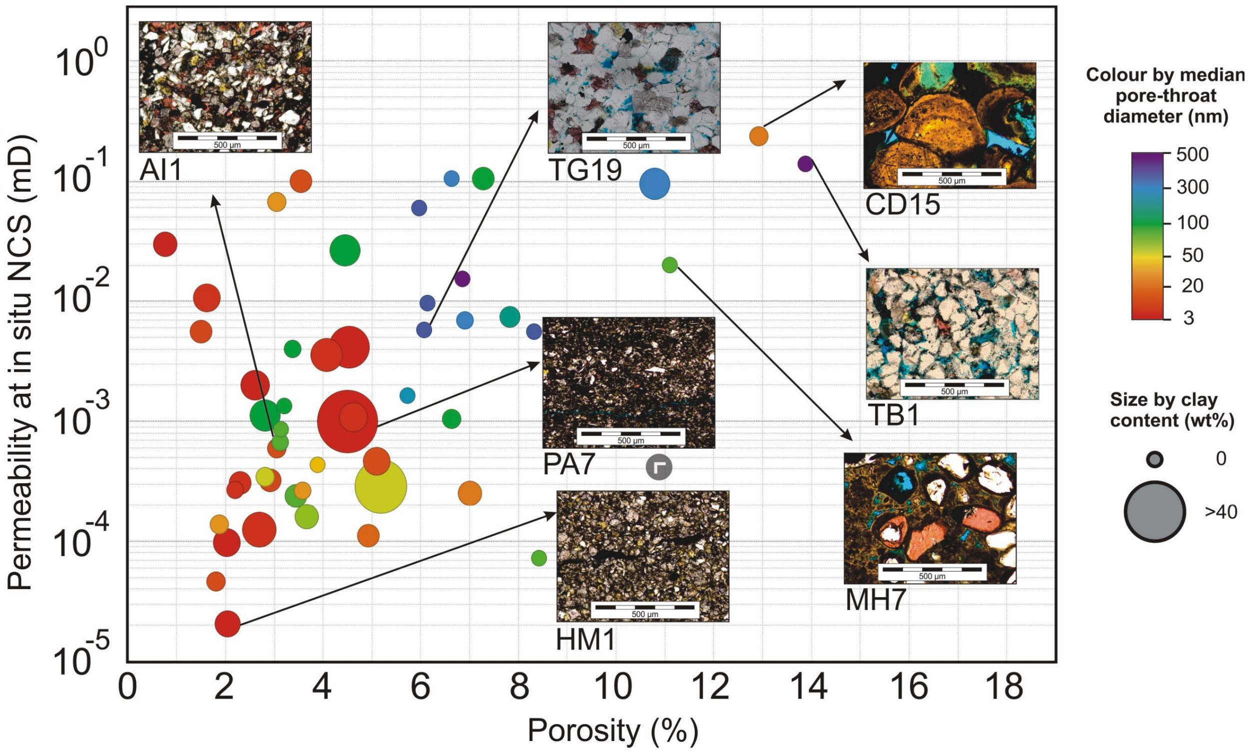

Figure 31. Crossplot of gas permeability at in situ net confining stress (NCS) versus porosity in samples analyzed for this study of the Doig Formation, northeastern British Columbia. Circle size is proportional to the total amount of clay and colour represents the median pore-throat diameter. Selected samples are highlighted to illustrate the textural variability, and its influence on porosity and permeability. Abbreviation: mD, millidarcy.

There is no relationship between permeability and total organic matter and mineralogy, with the notable exception of illite (clay) rich facies which invariably have low permeability (Figure 31). Any primary relationship that may have existed between composition and permeability is degraded by extensive carbonate replacement and cementation, in addition to elevated TOC values associated with relatively permeable phosphatic, oolitic packstone and grainstone lithofacies. Pore size distribution exerts a second order control on permeability. The highest permeability lithofacies have over 80% of their total pore volume accessible by pore throats larger than the macropore–mesopore boundary of 50 nm (Figure 33). The phosphatic, oolitic packstone and grainstone have pore-size distributions shifted toward the mesoporous region. However, the distributions are either broader or weakly bimodal, which enhances permeability, likely due to the interconnectedness of macropores through mesopores. This bimodality is a result of the presence of macropores produced by partial grain dissolution of ooids and mesoporous intergranular porosity. The low permeability rocks ($<10^{-3}$ mD) have 50% or more of their total pore volume accessible through the mesoporous region or finer and are composed mostly of finer grained siltstone with highly variable proportions of clay, carbonate in the form of cement and bioclasts, and organic matter.

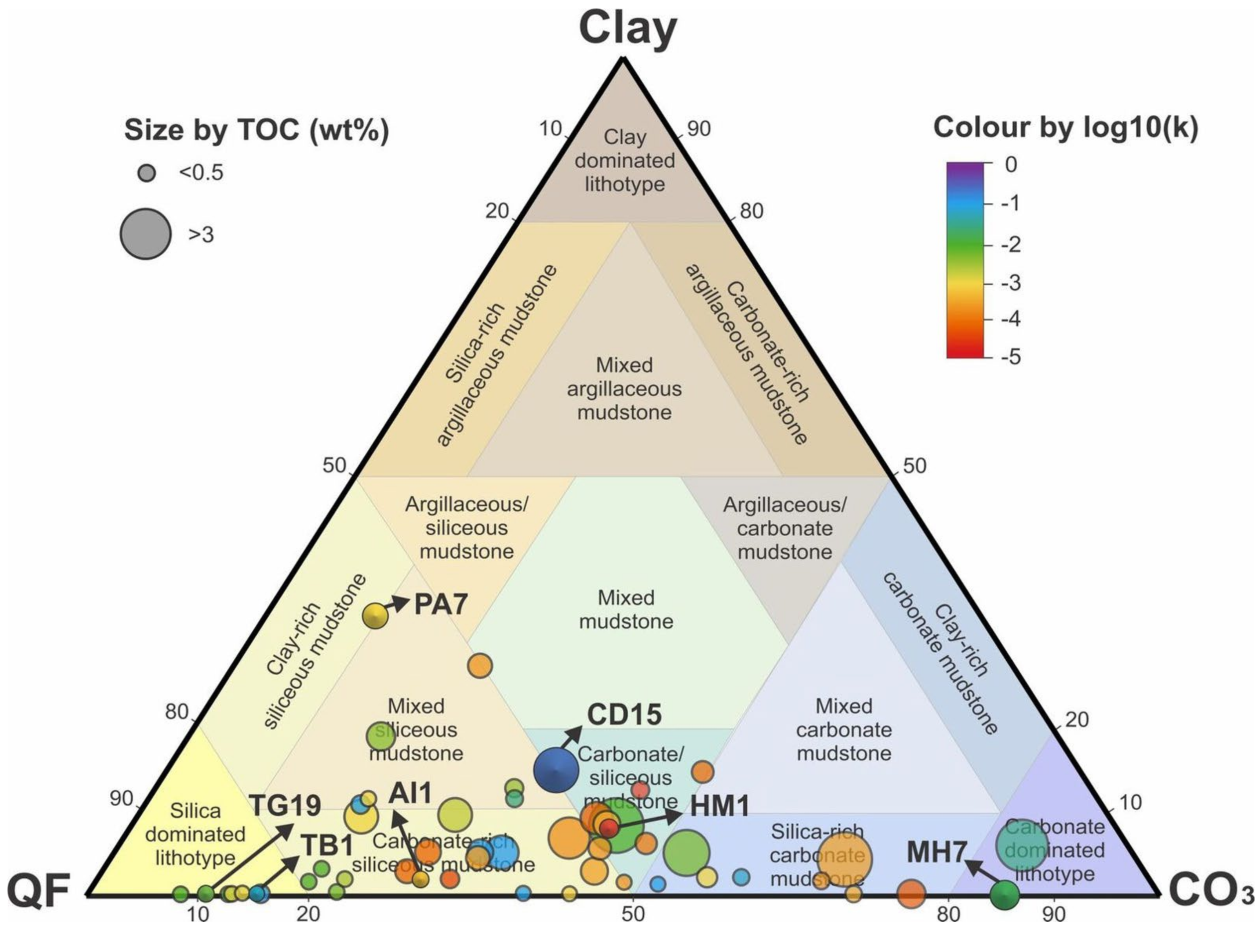

Figure 32. Ternary diagram of whole-rock mineralogy normalized to clay, carbonate and quartz-feldspar-plagioclase (QF; after Gamero-Diaz et al., 2012) of samples analyzed for this study of the Doig Formation, northeastern British Columbia. Total organic carbon (TOC) is represented by the size of the circles and the logarithm of gas permeability is represented as a colour gradient. Samples highlighted in Figures 30 and 33 are labelled.

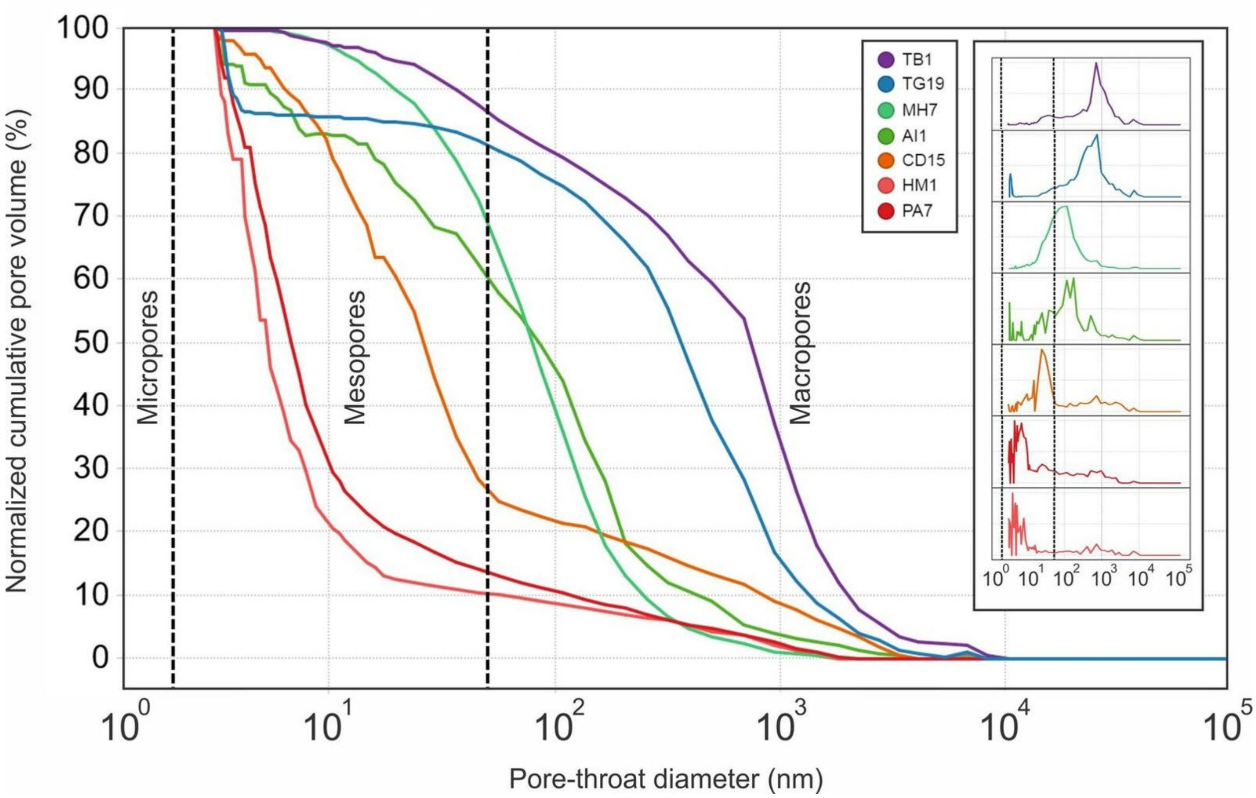

Figure 33. Curves of cumulative pore-throat diameter normalized to total pore volume of the selected samples highlighted in Figures 30 and 32. Inset shows their respective frequency distributions sorted by pore size, in descending pore size from the top.

References

Bailey, S. 2009. Closure and compressibility corrections to capillary pressure data in shales. Presented at the DWLS 2009 Fall Workshop, Colorado School of Mines, October 19.

Bailey, S., 2011, Closure and Compressibility Corrections to Capillary Pressure Data in Shales: presented at a meeting of the Canadian Well Logging Society, October 19.

Bustin, R. M. (1991): Organic maturity in the western Canada sedimentary basin; International Journal of Coal Geology, v. 19, p. 319–358.

Bustin, R.M. (1999): Organic maturity in the Peace River Arch area of the Western Canada Sedimentary Basin, Northeastern British Columbia; Canadian Society of Petroleum Geologists/Canadian Institute of Mining and Metallurgy in Digging deeper: finding a better bottom line; CSPG 99-12

Bustin, R.M. and A.M.M. Bustin (2016): Potential for natural-gas liquid from western Canadian shales: regional variation in thermal maturity and gas composition, northeastern British Columbia; in Geoscience BC Summary of Activities 2015, Geoscience BC, Report 2016- 1, p. 49–54.

Bustin, R.M., Munson, E., Letham, E. and Bustin, A.M.M. (2015): Quantification of the gas- and liquid-in-place and flow characteristics of shale and other fine-grained facies in northeastern British Columbia; in Geoscience BC Summary of Activities 2014, Geoscience BC, Report 2015-1, p. 89–94.

Carpentier, B., Huc, A.Y. and Bessereau, G. (1991): Wireline logging and source rocks - estimation of organic content by CARBOLOG® method; The Log Analyst, v. 32, no. 3, p. 279-297.

Comisky, J., M. Santiago, B. McCollom, A. Buddhala, and K. E. Newsham, 2011, Sample size effects on the application of mercury injection capillary pressure for determining the storage capacity of tight gas and oil shales: Society of Petroleum Engineers Canadian Unconventional Resources Conference, Calgary, Alberta 15-17 November, p. 1–23

Davis, M., and G. Karlen, 2013, A regional assessment of the Duvernay Formation; a world-class liquids-rich shale play: CSPG GeoConvention, Calgary, Alberta 6-12 May, p. 1-3.

Ferri, F. and Griffiths, M. (2014): Thermal maturity and regional distribution of the Muskwa Formation, northeastern British
Columbia; in Geoscience Reports 2014, BC Ministry of Natural Gas Development, p. 37–45.

Esptialié, J. (1986): Use of Tmax as a maturation index for different types of organic matter. Comparison with vitrinite reflectance; in Thermal Modeling in Sedimentary Basins, Exploration Research Conference Proceeedings, Orléans France, Editions Technip, p. 475–496.

Gamero-Diaz, H., Miller, C. and Lewis, R. (2012): sCore: A classification scheme for organic mudstones based on bulk mineralogy; American Association of Petroleum Geologists, AAPG South west Section Convention, May 19–22, 2012, Fort Worth, Texas, AAPG Search and Discovery article 40951, 18 p.

Hosseinian, A., Eberhardt, E. & Bustin, M. (2014). Hydro-mechanical behaviour of rough-walled fractures under shear offset: A 3-D numerical investigation. In DFNE 2014: 1st International Conference on Discrete Fracture Network Engineering, Vancouver, 19-22 October 2014. Edited by D. Kennard, D. Stead, E. Eberhardt & D. Elmo, CARMA/ARMA, e-Paper, DFNE 2014-157, 8 pp

Ibrahimbas, A. and Riediger, C.L., (2004): Hydrocarbon source rock potential as determined by Rock-Eval 6/TOC pyrolysis, northeast British Columbia and northwest Alberta; Resource Development and Geoscience Branch, Summary of Activities, pp.7–18.

Karst, R. and White, G. (1980): Coal rank distribution within the Bluesky-Gething stratigraphic horizon of northeastern British Columbia; in Geological Fieldwork 1979, a summary of field activities: Province of British Columbia, Ministry of Energy, Mines and Petroleum Resources Paper 1980-1: p. 103–107.

Letham, E.A. and Bustin, R.M. (2016): Apparent permeability effective stress laws: misleading predictions resulting from gas slippage, northeastern British Columbia; in Geoscience BC Summary of Activities 2015, Geoscience BC, Report 2016-1, p. 55–60.

MacLean, B.C. and Morrow, D.W. (2004): Bovie Structure: its evolution and regional context; Bulletin of Canadian Petroleum
Geology, v. 52, p. 302–324.

Munson, Erik & Chalmers, Gareth & Marc Bustin, R & Li, Kristal. (2016). Utilizing smear mounts for X-ray diffraction as a fully quantitative approach in rapidly characterizing the mineralogy of shale gas reservoirs. Journal of Unconventional Oil and Gas Resources. 14. 10.1016/j.juogr.2016.01.001.

Owen, J.N. and Bustin, R.M. (2017): Implications of the inorganic geochemistry of flowback water from the Montney Formation, northeastern British Columbia and northwestern Alberta: progress report; in Geoscience BC Summary of Activities 2016, Geoscience BC, Report 2017-1, p. 49–54.

Passey, Q.R., Creaney, S., Kulla, J.B., Moretti, F.J. and Stroud, J.D. (1990): A practical model for organic richness from porosity and resistivity logs; American Association of Petroleum Geologists Bulletin, v. 74, no. 12, p. 1777–1794.

Riediger, C.L., Fowler, M. G., Brooks, P. W. and Snowdon, L. R. (1990): Triassic oils and potential Mesozoic source rocks, Peace River Arch area, Western Canada Basin; Organic Geochemistry, v. 16, no. 1-3, p. 295–306.

Silva, P.L. and Bustin, R.M. (2017): Status report on petroleum system analysis study of the Triassic Doig Formation, Western Canada Sedimentary Basin, northeastern British Columbia; in GeoscienceBCSummary of Activities 2016, Geoscience BC, Report 2017-1, p. 25–28.

Silva, P.L. and Bustin, R.M. (2018): Preliminary liquid hydrocarbon potential assessment of the Doig Formation, northeastern British Columbia and west-central Alberta, based on thickness, organic richness and maturity; in Geoscience BC Summary of Activities 2017: Energy, Geoscience BC, Report 2018-4, p. 39–50.

Silva, P.L. and Bustin, R.M. (2019): Variability and controls on the matrix permeability of the Doig Formation in northeastern British Columbia; in Geoscience BC Summary of Activities 2018: Energy and Water, Geoscience BC, Report 2019-1, p. 21–28.

Stasiuk, L. D. and M. G. Fowler, 2002, Thermal maturity evaluation (vitrinite and vitrinite reflectance equivalent) of Middle Devonian, Upper Devonian, and Mississippian strata in the Western Canada edimentary basin: Geological Survey of Canada, Open file 4341.

Unrau, S. and Nagel, B. (2012): Using compositional gas data for horizontal drilling and practical detection of natural gas liquids

(NGL); Canadian Society of Petroleum Geologists, GeoConvention 2012, May 14–18,2012, Calgary, Alberta, extended abstract, 4 p.

Walsh, W., Adams, C., Kerr, B. and Korol, J. (2006): Regional “shale gas” potential of the Triassic Doig and Montney formations, northeastern British Columbia; BC Ministry of Energy and Mines, Oil and Gas Division, Resource Development and Geoscience Branch, Petroleum Geology Open File 2006-02, 19 p.

Wilson, T.K. and Bustin, R.M. (2017): Unconventional petroleum systems analysis of Upper Devonian organic-rich shale units in the Horn River and Liard basins, northeastern British Columbia and adjacent western Alberta: preliminary report; in Geoscience BC Summary of Activities 2016, Geoscience BC, Report 2017-1, p. 29–36.

Wilson, T.K. and Bustin, R.M. (2018): Regional variability of reservoir properties of the Devonian shales of northeastern British Columbia; in Geoscience BC Summary of Activities 2017: Energy, Geoscience BC, Report 2018-4, p. 51–64.

Wilson, T.K. and Bustin, R.M. (2019): Basin modelling and thermal history of the Horn River and Liard basins, Cordova Embayment, and adjacent parts of the Western Canada Sedimentary Basin; in Geoscience BC Summary of Activities 2018: Energy and Water, Geoscience BC, Report 2019-1, p. 1–20